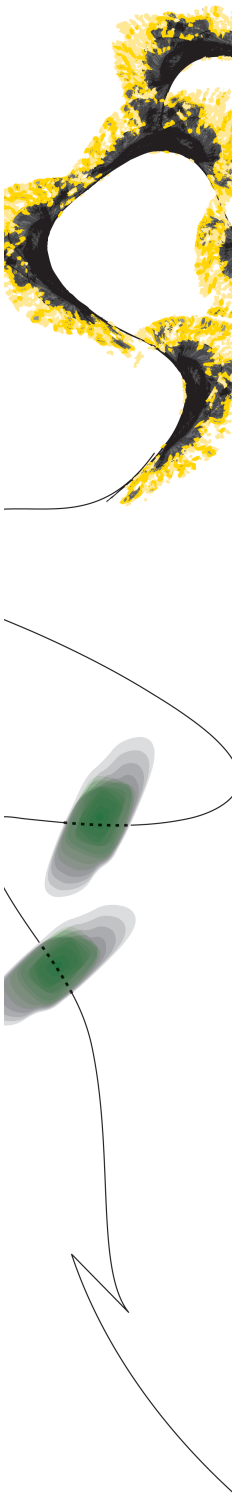

Catalase-laden oxygen-generating constructs as potential artificial erythrocytes

Master Thesis Biomedical Engineering

Indra Mooij

Examination committee:
MSc. F. L. F. Gomes
Dr. J. C. H. Leijten (Chair)
Prof. Dr. Ir. P. Jonkheijm
Prof. Dr. A. D. van der Meer

Developmental BioEngineering & Molecular NanoFabrication
Biomedical Engineering - Bioengineering Technologies
Faculty of Science and Technology
University of Twente
Enschede, the Netherlands

November 24, 2023

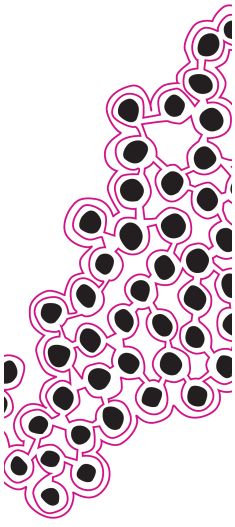

UNIVERSITY OF TWENTE.

1 Abstract

Introduction Blood transfusions are indispensable in clinical practice. Unfortunately, the blood supply is scarce and donor-dependent. Strict donor eligibility criteria, blood type matching, low availability of the universal blood type, and the short shelf-life of blood products put a further strain on the scarcity of blood. The blood supply is labile, and therefore, blood substitutes are heavily sought after. Blood substitutes can be engineered in such a way that universality, safety, easy storage conditions, and most importantly, scalability, can be taken into account.

Methods In this work, an erythrocyte substitute based on calcium peroxide (CPO) is developed. CPO is embedded in polycaprolactone (PCL), a hydrophobic polymer that sustains the release of oxygen (O_2). CPO generates oxygen through hydrolytic degradation. An antioxidant, catalase, is added to decrease the generation of reactive oxygen species. Catalase is a protein that is responsible for the degradation of hydrogen peroxide (H_2O_2) into oxygen and water, thereby ensuring protection of cells against oxidative stress. Erythrocyte-inspired lipid coatings are added to increase the hemocompatibility of the constructs. In this research, it was evaluated how catalase can be incorporated in OG-PCL microparticles and what its effect is on the H_2O_2 and O_2 release kinetics. Two different erythrocyte-inspired lipid coatings have been added and compared in terms of hemocompatibility. Additionally, it was assessed whether the addition of a lipid membrane has adverse effects on the catalase.

Results and conclusion OG-PCL microparticles were produced at small sizes. Minor amounts of CPOs were able to be encapsulated. H_2O_2 and O_2 release was detected for up to 48 hours, however, the measurement methods had various limitations. CO-OG-PCL MPs were produced by coating OG-PCL MPs with a catalase layer. Although the association efficiency of catalase with PCL was low, the antioxidizing capacities of the catalase were evident by flattening out an initial, cytotoxic burst release of H_2O_2, which was observed in constructs without catalase. Two complex lipid formations, IT and PT (a PEGylated variant of IT) were compared in terms of hemocompatibility through C5a and IgG activation assays and in a cell viability study. PT-coated CO-OG-PCL MPs induced the lowest immune response, despite not being formed properly on CO-OG-PCL. The addition of catalase limited the complexity of the lipid coating formulations, as lipids with high melting temperatures could not be used,as heating denatured the catalase. A new, less complex CT lipid formulation was included, which was able to coat CO-OG-PCLs properly due to lower melting temperatures of the lipids. It is encouraged to continue further work with this lipid formulation and to explore other materials and protocols to obtain higher encapsulation rates of CPOs and catalase in the substrates.

2 Samenvatting

Introductie Bloed transfusies zijn onmisbare ingrepen in de medische wereld. Echter, de hoeveelheid donorbloed is schaars en afhankelijk van vrijwillige donaties. Er zijn strenge criteria waaraan een donor moet voldoen. Daarnaast is het cruciaal om bloedgroepen te matchen en komt de universele bloedgroep te weinig voor voor de grote vraag. Tenslotte hebben bloedproducten een gelimiteerde houdbaarheidsdatum na donatie. Deze factoren onderstrepen de nood voor een kunstmatig alternatief voor donorbloed. Bloed alternatieven kunnen op zodanige manier bedacht worden dat ze universeel, veilig, lang houdbaar en gemakkelijk opschaalbaar zijn.

Methode In dit onderzoek is een erythrocyt-alternatief gebaseerd op calcium peroxide (CPO) gemaakt. CPO deeltjes werden ingesloten in een matrix van polycaprolactone (PCL), een hydrofobe polymeer die ervoor zorgt dat de zuurstof generatie langzamer verloopt. CPO genereert zuurstof (O_2) wanneer het in contact komt met water doormiddel van hydrolytische degradatie. Tijdens deze reactie komen vrije zuurstof radicalen vrij. Een antioxidant, catalase, werd toegevoegd om dit te verminderen. Catalase is een eiwit dat van nature voorkomt in erythrocyten en katalyseert de omzetting van waterstof peroxide (H_2O_2) naar O_2. Door deze katalysatie vermindert de hoeveelheid H_2O_2 en zijn de uiteindelijke deeltjes minder cytotoxisch. In dit onderzoek is onderzocht hoe catalase het best kan worden toegevoegd aan de zuurstof-genererende deetjes en wat het effect van catalase is op de generatie van H_2O_2 en O_2. Synthetische celmembranen, gebaseerd op het natuurlijke celmembraan van een erythrocyt, werden toegevoegd om de hemocompatibiliteit van de deeltjes te verbeteren. Twee verschillende coatings werden toegevoegd en vergeleken doormiddel van hemocompatibiliteitstesten. Daarnaast werd onderzocht of de toevoeging van een synthetisch celmembraan negatieve effecten heeft op de werking van catalase.

Resultaten en conclusie Kleine zuurstof-genererende microdeeltjes (OG-PCL MPs) werden gemaakt met lage hoeveelheden CPO. H_2O_2 en O_2 generatie werd gemeten gedurende 48 uur, maar slechts in kleine getalen. OG-PCL MPs met catalase (CO-OG-PCL MPs) werden gemaakt door incubatie met catalase aan het oppervlakte van de MPs. De efficientie van deze methode was laag, maar de werking van catalase was aantoonbaar in de H_2O_2 metingen. Twee synthetische celmembranen (IT en PT) werden vergeleken met betrekking tot de hemocompatibiliteit, doormiddel van C5a en IgG activatie en cell viability (levensvatbaarheid). PT-CO-OG-PCL MPs hadden over het algemeen de hoogste hemocompatibiliteit, hoewel de coatings niet goed gevormd waren. Dit komt doordat de formuleringen vetzuren met hoge smelttemperaturen bevatte. Catalase kan niet verhit worden tot hogere temperaturen zonder te denatureren, daarom is er een nieuwe formulering die niet verhit hoefde te worden onderzocht. Deze CT formulering vormde mooie, stabiele coatings om de MPs. Het word aangeraden om verder onderzoek voort te zetten met deze formulering en om andere substraten en protocollen voor de incorporatie van CPO te onderzoeken.

Table of Contents

List of Abbreviations

ABC Accelerated blood clearance

CARPA Complement-activation-related pseudoallergy
CPO Calcium peroxide

DCM Dichloromethane
DOPC 1,2-Dioleoyl-sn-glycero-3-phosphocholine

EDX Energy dispersive X-ray spectroscopy
ELISA Enzyme-linked immunosorbent assay

HBOC Hemoglobin-based oxygen carrier
HP Hemolysis percentage
HRP Horseradish peroxidase
HUVECs Human umbilical vein endothelial cells

LP Liquid peroxide
LPS Lipopolysaccharides

MQ Milli-Q water

OCB Oxygen-carrying biomaterial
OGB Oxygen-generating biomaterial

PC Phosphatidylcholine
PCL Polycaprolactone
PEG Polyethylene glycol
PFC Perfluorocarbon
PI Phosphatidylinositol
PLA Polylactic acid
PO2 Partial oxygen pressure
PS Phosphatidylserine

RBC Red blood cell
ROS Reactive oxygen species

SALB Solvent-Assisted Lipid Bilayer
SEM Scanning electron microscopy
SM Sphingomyelin
SOD Superoxide dismutase
SP Solid peroxide

TTI Transfusion-transmitted infection

WCA Water contact angle

3 Theoretical background

In this chapter, theoretical background information necessary for obtaining a thorough understanding of the clinical problem and the state of the art of oxygen therapeutics is given. The immune response to intravenously delivered microparticles is described, as it is crucial to understand in order to design a hemocompatible therapy.

3.1 The scarcity of donor blood

Almost all tissues need oxygen to survive. Oxygen is necessary for cells to carry out their basic metabolic functions. When the oxygen supply is limited or unavailable, tissues can become damaged and their function impaired. In the human body, oxygen is carried and delivered to the tissues by blood. Blood consists of three primary components, namely plasma, accounting for approximately 55% of the blood volume, white blood cells and platelets, constituting less than 1% of the total blood volume, and erythrocytes, or red blood cells (RBCs), which make up 40-45% of the total blood volume [4]. Each component serves specific functions within the bloodstream. Erythrocytes are responsible for transporting up to 98% of the oxygen in the body to the tissues, the remainder of oxygen is dissolved in the plasma [26]. Because blood enables the oxygenation of tissues, and essentially, life, blood has been described as red gold [4].

In certain conditions such as anemia, hemophilia, or other blood-related disorders, the body is incapable of producing healthy blood. Patients suffering from these conditions often require blood transfusions. Transfusions are also essential after major blood loss caused by trauma or surgery, and ensure that tissues and organs do not become damaged as a result of long-term hypoxia. Therefore, blood transfusions are indispensable in hospitals. It is estimated that about 50% of patients that present at the emergency department need blood transfusions [4]. The blood is donated by volunteers at blood banks and can be stored as whole blood, or separated into different components. The storage conditions of blood are one of the challenges that are faced with donor blood. Platelets can only be stored for up to 5 days, and need to be at constant agitation in specialized equipment. Plasma can be frozen for up to 18 months, but once thawed, must be used within 24 hours. Erythrocytes can be stored for up to 42 days in refrigerated conditions. Over time, they can contract storage lesions, which damage the morphology and performance of the erythrocytes, once transfused [5]. The storage requirements of blood make it difficult to transport blood to remote and less developed locations. Next to these challenges, blood banks have strict criteria that a donor should meet, to ensure blood safety and to minimize the risk of transfusion-transmitted infections (TTIs). TTIs are infections that can be passed from one individual to another through blood transfusions. These can range from bacterial infections to parasitic and viral diseases, including Ebola, Hepatitis, West Nile Virus and variant Creutzfeldt-Jakob Disease [45, 68]. The emergence of Human Immunodeficiency Virus in 1980 called for rigorous donor blood testing, and as a result, in Western countries, the risk of TTIs is minimal. However, in developing countries, there is a lower budget for blood testing, resulting in lower-quality donor blood. Additionally, the blood donation rate is significantly lower in low-income countries (5/1000 inhabitants) compared to high-income countries (31.5/1000 inhabitants), while these countries are inhabited by 80% of the world's population [4, 34, 45, 68].

The demand for blood transfusions is escalating due to population growth and aging, posing a significant healthcare challenge [10]. The global blood supply is donor-dependent and unstable. The supply can easily be disrupted, resulting in a blood shortage. This problem became evident to the general public during the recent COVID-19 crisis [39]. Insufficient blood donations during the pandemic led to the postponement of surgeries and medical treatments. Other events, such as natural disasters and wars, can locally disrupt the blood supply. Frequent donations of all blood types are necessary to ensure a stable supply. Especially the universal blood donor type, O-, is in

constant high demand. O- can be safely administered to any patient, due to its lack of Rh and ABO antigens on the surface.

All of these problems highlight the persisting need for blood substitutes, a need that has been around since the discovery of blood circulation in 1628 by William Harvey [45]. However, a whole blood substitute is not feasible in the current day and age. Hence, researchers have focused on substituting the one component of blood that facilitates the gas exchange, namely RBCs. Artificial RBCs can be designed to avoid limitations that are faced with donor blood. The requirements an ideal RBC replacement should meet must include the ability to transport oxygen and scavenging of carbon dioxide, prolonged oxygen release, no need for crossmatching, minimal risk of contamination and TTIs, no toxicity, an appropriate half-life in circulation, no accumulation in various tissues, easy and low-cost production, and the substitutes should have easy storage conditions [10, 34, 45].

3.2 Current state of the art in blood substitution

Various studies have attempted to create erythrocyte replacements. These therapies are called RBC substitutes, or oxygen therapeutics. Three categories are often distinguished: stem cell-derived oxygen therapeutics, oxygen-carrying biomaterials (OCBs) and oxygen-generating biomaterials (OGBs). These will be discussed in the following sections.

3.2.1 Stem cell-derived oxygen therapeutics

Stem cell-derived oxygen therapeutics or bio-engineered RBCs, are based on the *in-vitro* differentiation of stem cells into RBCs, before transplantation back to the patient. Various stem cell types, including induced pluripotent stem cells, hematopoietic stem cells, umbilical cord cells, and other stem cell types have been used for this approach [4, 45, 63]. Multiple studies have correctly differentiated stem cells into adult RBCs, which could reversibly bind and release oxygen [19, 63]. Unfortunately, stem cell-based oxygen therapeutics are donor- and blood-dependent, making it difficult to upscale to a level at which this therapy becomes a feasible alternative to donor blood. Additionally, stem cell differentiation is expensive.

3.2.2 Oxygen-carrying biomaterials

Hemoglobin-based oxygen carriers (HBOCs) are oxygen-carrying biomaterials (OCBs) that can reversibly bind oxygen, using natural hemoglobin or myoglobin. Myoglobin and hemoglobin are heme proteins, which can reversibly bind oxygen. Myoglobin is found in skeletal muscle and has one oxygen binding site, as opposed to hemoglobin, which is found in erythrocytes and has four oxygen binding sites [2]. HBOCs are designed to encapsulate hemoglobin or myoglobin within a biocompatible carrier. The binding and release of oxygen is dependent on the physiological partial oxygen pressure in the environment (PO2) [45, 67]. HBOCs can reversibly bind and release large amounts of oxygen, but the oxygen is released without adequate control and within a short time frame. Additionally, the constructs generally have short circulation times [45, 67]. HBOC trials have faced side effects like myocardial infarction, kidney failure, stroke, and an increased mortality rate [9, 45, 67]. This is thought to be caused by HBOC-associated nitric oxide scavenging and toxicity related to the polymerization and breakdown of the hemoglobin tetramer to hemoglobin dimers and monomers [9, 10, 26, 54]. Hemoglobin detaches from the constructs, inducing toxicity. To prevent this, multiple studies have worked with cross-linked, polymerized, and conjugated hemoglobin [45]. These modifications render the hemoglobin less likely to detach [45]. DCLHb HemAssist, a cross-linked HBOC, has reached phase III clinical trials, but was found to increase mortality rates. Various complications, such as arterial hypertension, gastrointestinal side effects, and yellow skin discoloration were observed [45, 55]. Polymerized HBOCs also faced other side effects, such as increased risk of cardiovascular

problems, increased risk of myocardial infections and overall high mortality rates [45]. Additionally, HBOCs rely on blood-based materials. This defeats the purpose of an alternative to donor blood. Some studies have used hemoglobin from animal sources to overcome this. However, using hemoglobin from animal sources can pose other serious risks, namely prion diseases [9, 10]. Despite efforts to overcome the limitations of HBOCs by modifying and using hemoglobin from animal sources, HBOCs are currenly not an ideal candidate for a RBC subsititute.

Perfluorocarbon-based oxygen carriers are chemically and biologically inert perfluorocarbon (PFC) emulsions. They are fully synthetic, gas-dissolving liquids which are not metabolized and insoluble in the aqueous phase. Because they are heat resistant, they can be easily sterilized by heat [9, 10, 45]. PFC emulsions can dissolve more oxygen than water, up to an oxygen concentration of 40-50% [45]. Since PFCs can also dissolve CO_2, they are interesting materials for respiratory gas transport. PFCs are one of the oldest oxygen therapeutics in the field and have been researched extensively, with one of the earliest formulations, Fluosol, reaching the market in 1989. However, the formulation was removed again in 1994, due to clinical problems resulting in inflammation, and low therapeutic effect [10]. The duration of the oxygen release was short and poorly controlled, the majority was released before the PFCs reached the microvasculature [10]. Next to low therapeutic effect, some studies have faced organ retention of PFCs, attenuated immune responses, and complement activation [9, 10, 27]. Second-generation PFCs contained modifications to prevent organ retention, but oxygen delivery was still less than 30% compared to blood transfusions. In some countries, such as Russia, Mexico, and South Africa, the second-generation formulation Perftoran® (Vidaphor) is currently on the market for specific applications, such as enhancing transplant survival and plastic surgery [9, 10]. However, the FDA has not approved the therapy because of a lack of clinical evidence [10, 27]. As of now, PFC formulations are still being researched in several clinical trials for different applications, including RBC substitution.

3.2.3 Oxygen-generating biomaterials

Oxygen-generating biomaterials (OGBs) are oxygen releasing constructs, often consisting of multiple materials. The oxygen-generating components can be embedded in substrate materials in order to improve the release kinetics and delivery of the constructs. These constructs are referred to as OGBs.

One of the most promising mechanisms in OGBs is the usage of liquid or solid peroxides (LPs and SPs). LPs and SPs are chemical compounds that contain a peroxide group. This group is highly reactive and can easily be broken, releasing reactive oxygen species (ROS), which can be further decomposed to oxygen. The oxygen release is dependent on the temperature, solubility, pH, and the presence of catalysts [18, 58]. Examples of SPs that are used in OGBs are calcium peroxide (CPO), magnesium peroxide, and sodium percarbonate [18, 51, 58, 67]. Oxygen is generated when SPs interact with water and undergo hydrolytic degradation (equation 1 for CPO). Hydrogen peroxide (H_2O_2) is formed first, which decomposes into oxygen. The final conversion from H_2O_2 to O_2 is shown in Equation 2.

$$CPO : \mathrm{CaO_2\,(s)} + 2\,\mathrm{H_2O} \longrightarrow \mathrm{Ca(OH)_2} + \mathrm{H_2O_2} \tag{1}$$

$$2\,\mathrm{H_2O_2} \longrightarrow \mathrm{O_2} + 2\,\mathrm{H_2O} \tag{2}$$

The oxygen release of SPs is slower than that of LPs, as SPs are solid at room temperature and less soluble in water. However, the release remains too abrupt for clinical applications. As a result of the fast-paced hydrolysis, high levels of ROS can be generated [67]. This can induce cytotoxicity

[18, 67]. In order to sustain the release of both oxygen and ROS, SPs can be embedded in substrate materials, which reduce the rate of hydrolysis. Hydrophobic materials, such as polydimethylsiloxane, poly(lactic-co-glycolic acid), and polycaprolactone (PCL) are often employed for this. To further decrease the amount of ROS that is generated by the constructs, antioxidants can be added. Antioxidants are free-radical and ROS scavenging proteins [18, 58, 67]. More information about ROS-induced cytotoxicity and the role of antioxidants is given in section 3.3.4. Various studies are being conducted on peroxide-based OGBs. Some limitations that have been found include burst release of peroxide-byproducts, cytotoxic effects, and short-term oxygen release [18]. Different types of polymers and hydrogels are being researched for the optimization of peroxide-based OGBs, as well as surface modification methods to achieve longer circulation times and immunosuppression. It is important to note that OGBs introduce new oxygen into the body. This should be taken into consideration when determining dosages and when thinking of clinical applications for these therapeutics. Additionally, since peroxide-based OGBs are typically larger than PFCs, there is a risk of obstruction of capillaries and accumulation in tissues and organs. This can have serious consequences, including stroke or even death. The particle size and the deformability of the constructs is extremely important when designing these constructs.

In conclusion, OGBs have the advantage of possessing a higher oxygen payload than other oxygen therapeutics, and release oxygen independent of the PO2. It is possible to encapsulate the oxygen-generating elements in substrates to achieve a fine-tuned release profile and to decrease ROS-induced cytotoxicity. Additionally, OGBs can be modified to acquire prolonged intravenous circulation times. By using these modifications, some studies have reported that the oxygen release of SPs can be sustained for multiple days [15, 51]. This is very relevant for its purpose as a RBC substitute. Because antioxidant-containing, substrate-embedded SPs are one of the most promising candidates in the field of oxygen therapeutics right now, this is the principle on which oxygen-generating constructs in this research are based.

3.2.4 Applications of oxygen-releasing therapeutics

The main envisioned application of these OGBs is as RBC substitutes in blood transfusions. The urgency of this application is highlighted in section 3.1. However, since this is a systemic application and OGBs are still in earlier stages of research, it is possible that the therapy is approved for other, less invasive, and localized applications first. It might not be realistic that the therapy will completely substitute donor blood. Other components, such as plasma, white blood cells, and platelets are not substituted in this therapy. These levels must be also regulated after blood loss. Therefore, OGBs could be administered in addition to blood products as a combination therapy, which still decreases the necessary amounts of scarce donor blood.

Examples of localized applications of OGBs are inschemic tissues. Localized administration of OGBs, for example by incorporation in scaffolds or grafts, can help prevent further progression of or even recover ischemia by delivering oxygen directly to the tissue. Another example of localized therapy is the oxygenation of solid tumors, which increases their susceptibility to radiotherapy and chemotherapy [33].

Furthermore, OGBs are extremely interesting for tissue-engineering. It is not surprising that they are already being utilized in this field [15, 18, 58, 62]. The limit of diffusion and the inability to initialize and mimic proper vascularization is a huge limitation in tissue engineering. Because of this, tissue-engineered constructs have a size limitation. Larger 3D constructs will form a necrotic core as a result of hypoxia. Embedded OGBs can oxygenate the implants from within and aid the process of neovascularization of the implant or tissue. This can result in increased implant survival rates. For example, Touri et al. have been able to increase the level of oxygen and cell survival rates in 3D printed bone tissue-engineered scaffolds by using CPO-based OGBs [62]. OGBs are not

only interesting for tissue-engineered constructs, but also for human-sourced implants, such as skin grafts or organs. An example is during the transplantation of isolated islets of Langerhans. The naturally occuring angiogenesis after the transplantation is not sufficient to support the high oxygen demand of the cells, and therefore, patients receive supplemental oxygen through injected probes. OGBs can be incorporated during the transplantation of the islets to enhance the islets' survival rates [58]. Another example, regarding wound healing, is a study by Harrison et al., in which sodium percarbonate-based OGBs were incorporated into wound healing films to investigate their role in rats to reduce flap necrosis [21]. Next to *in-vivo* applications, OGBs can be utilized in perfusion systems during organ transport for organ transplantations. This could increase the organ survival time *ex-vivo* and decrease the damage the organ faces during transport.

3.3 The immune response to intravenous microparticles

RBC substitutes are administered intravenously. Upon delivery, the immune system will be activated, with the goal of eliminating these foreign objects from the body, essentially neutralizing them before fulfilling their purpose. Therefore, the immune response is crucial to understand in order to design a construct with minimal immunogenicity.

3.3.1 The immune response to microparticles in short

Upon arrival in the bloodstream, the immune response to foreign objects typically consists of several phases. These are shown schematically in Fig 1. The events of each phase are discussed below [56].

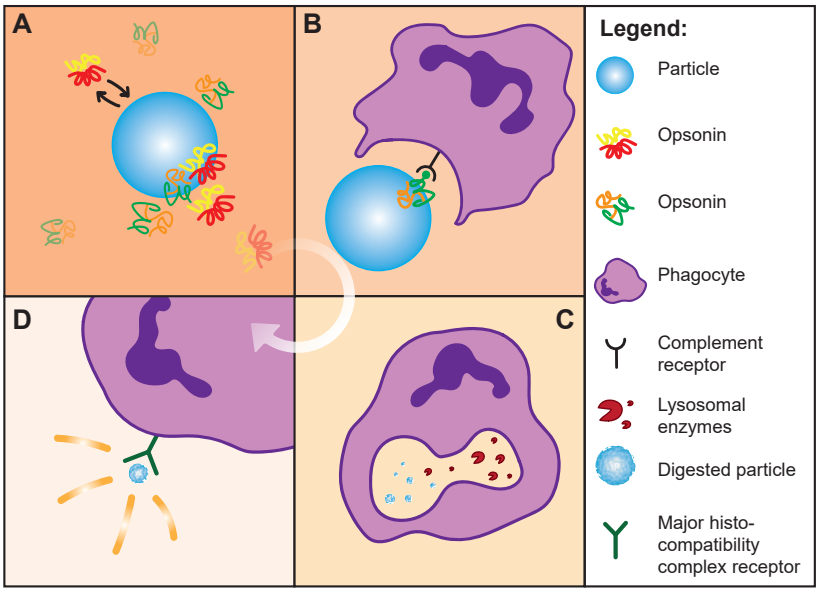

Figure 1 *The immune response to intravenously delivered particles in short. **A** Opsonization **B** phagocytosis, **C** digestion, and **D** antigen presentation.*

1) **Opsonization:** Opsonization is the first response after the particles enter the bloodstream. Specific proteins, called opsonins, bind to the surface and form a protein corona. This is a shell of proteins, marking the particle for recognition by immune cells. These proteins come from the surrounding blood plasma. The protein corona plays a crucial role in determining the particle's interactions with the body. A part of the corona is dynamic and changes in response to variations in the surrounding medium, such as changes in composition, pH, or temperature [17]. Some proteins might attract each other, further enriching the protein corona's composition, while others can exchange with proteins from the plasma [17]. It is important to note that not all proteins in the protein corona are opsonins. Some proteins, known as dysopsonins or stealth proteins, help avoid immune system recognition. Examples of dysopsonins include lipoproteins and human serum albumin [48]. Dysopsonins downregulate the phagocytosis of particles by immune cells. There are methods to influence the formation or reduce the formation of the protein corona [57]. These will be discussed in section 3.3.2.

   The **complement protein cascade** is also initiated during this phase. This is a chain of reactions in the first line of defense of the body and one of the largest challenges in nanomedicine [56]. The cascade is intended to rapidly clear pathogens out of the system. Particles are recognized as foreign, and thus, activate the complement cascade. Results are

decreased circulation times and decreased therapeutic effect. The complement system consists of three different pathways, namely the classical, alternative, and lectin pathways, each dependent on specific activators [36, 56, 64]. Based on the pathway, complement protein C3 is activated and cleaved. C3a is an anaphylatoxin and can be used as a biomarker to determine complement activation. C3b forms covalent bonds with the surface of the particle and marks it for recognition by phagocytes, by binding on the complement receptors on phagocytes (see Fig. 1). It also recruits other proteins to form the enzymatic complex C5 convertase. C5 convertase cleaves complement protein C5 into C5a and C5b. These are also anaphylatoxins and stimulate immune cells to release inflammatory mediators, such as histamine. As a result, this process can lead to anaphylactoid syndrome or complement-activation-related pseudoallergy (CARPA) [32, 56, 64]. CARPA will be discussed further in section 3.3.3

2) **Phagocytosis:** Once the particles are opsonized, phagocytes recognize and bind to the opsonized particles through their cell surface receptors, such as the FcRn and C3 receptors [48]. These receptors have a high affinity for the opsonins present on the particle surface. As a result of this binding, the particle is engulfed in a vesicle, called the phagosome [32, 36, 56, 57].

3) **Digestion:** Intracellularly, phagosomes fuse with lysosomes. Lysosomes contain digestive enzymes that break down the contents of the phagosome, including the particles [48, 56]. The particle is neutralized. Intracellular components, such as the catalase and the CPO, will also be digested.

4) **Antigen presentation:** The breakdown products of the phagosome, also called antigens, are presented on the surface of antigen-presenting cells, such as dendritic cells, macrophages and monocytes. This is done using the major histocompatibility complex [56].

5) **Adaptive immune response:** More complex immune cells, such as B- and T-cells, recognize the antigens. This recognition initiates the adaptive immune response to the particles. B-cells produce antibodies that bind to the surface of the particles and mark them for recognition by killer T-cells. Memory B and T-cells provide long-term immunological memory against the specific antigens of the particles. When the particle is administered again, these cells facilitate a quick and more elevated immune response, as the right immune cells as recruited right away [36, 56]. These memory cells can be against specific materials of the particle.

3.3.2 Surface modification methods to minimize the immune response

The constructs in this thesis are based on CPO, which is embedded in a PCL matrix with catalase as an antioxidant. These variables are important to identify, as the choice of materials affects the immune reaction. As PCL is a hydrophobic polymer, it has a tendency to aggregate and flocculate in aqueous surroundings, including blood. To overcome this, erythrocyte-inspired lipid coatings are added. These lipid coatings modify the surface of the particles. Surface modifications can also be used to decrease the rate of opsonization, as the surface is what determines the composition of the protein corona. There are multiple methods to minimize the immune response to particles. An adequate method will extend circulation times, and increase the efficacy of the particles. Numerous techniques and materials can be used for surface modification. In this section, two techniques that are relevant for this research will be discussed. They can be used in addition to lipid coatings on the PCL.

One of the most frequently used surface modifications is the addition of polyethylene glycol (PEG). This process is referred to as **PEGylation**. PEGylation is considered the gold standard of surface modifications for reducing the rate of opsonization [61]. PEG is a polyethylene glycol polymer chain of n repeats, as seen in Fig. 2. Multiple possible lengths of the polymer chain exist,

based on the molecular weight of the formulation. PEG is widely accepted as biocompatible, although recently, more and more concerns are being raised on this matter, which will be discussed in section 3.3.3. The polymer chains form a hydrophilic coating on the particle, disrupting the formation of the protein corona by steric hindrance [70]. This can be seen in Fig. 2. As a result, immune cells are less likely to identify and neutralize the particles. This is referred to as an anti-fouling capability. When the molecular weight of PEG increases, and the chains get longer, the anti-fouling capacity increases. PEG has been proven to extend circulation times and enhance the therapeutic window of encapsulated drugs [32, 36, 70]. Numerous PEGylated drug formulations are currently approved and on the market, such as Doxil® (Doxorubicin), Onivyde® (Irinotecan) and the recent COVID vaccines by Pfizer-BioNTech and Moderna [32]. PEGylation is a relatively easy process and is suitable for many different kinds of agents, such as small molecules, peptides, proteins, particles and liposomes [61]. In this thesis, PEGylation is utilized to enhance the circulation times and to minimize the immune response against the OGBs.

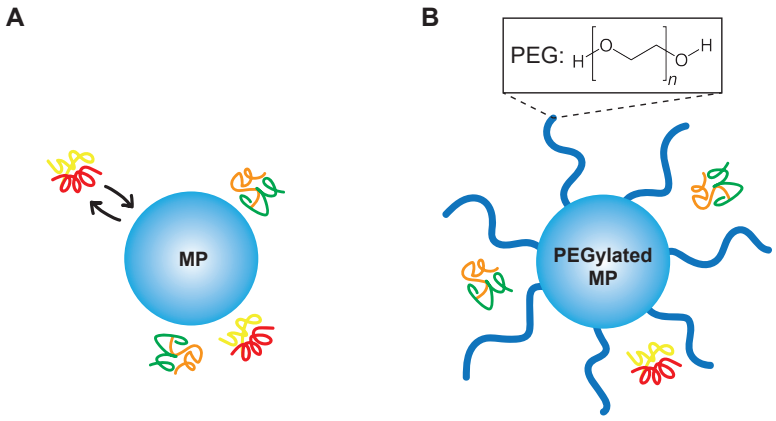

Figure 2 *PEGgylation lowers the rate of opsonization of microparticles (MPs) by steric hindrance.* ***A*** *The formation of the protein corona on non-PEGylated MPs in plasma* ***B*** *PEGylation minimizes the formation of the protein corona by steric hindrance.*

Another surface modification method that can minimize the immune response is the usage of **ghost membranes** or **artificial cell membranes**. A ghost membrane is the cell membrane of a biological cell, which is extracted or detached from the cell by sonication, extrusion, or a combination of both techniques [26]. Regarding erythrocytes, the erythrocyte membrane can be used as a coating for nano- and microparticles, such as HBOCs or PFCs. Upsides of this surface modification technique are that the membrane is nearly identical to that of native erythrocytes, resulting in good biocompatibility and similar biological interactions with the environment as erythrocytes. The membranes can be altered with other additives, such as PEG, to achieve better stability and circulation times [26, 57]. However, extracting ghost membranes requires donated erythrocytes, which are scarse. The cell membrane can also be damaged during extraction and lysis, which can be seen as a waste of valuable erythrocytes that could otherwise have been used in transfusions. Batch-to-batch variability is also an issue when using biological materials. Since this technique is blood-dependent, it is not a scalable surface modification method.

Artificial cell membranes work by replicating the cell membrane as closely as possible with synthetic materials. These are also called *biomimetic* or *bio-inspired* coatings. The incentive is that since the artificial bilayer is similar to the biological bilayer, the immune system should not recognize the particle as foreign [26, 57]. In reality, it is near impossible to completely mimic the exact composition of a particular cell membrane, so an immune response will not be absent, but much less pronounced. Synthetic lipid cell membranes are not extensively explored yet as particle

coatings, but could potentially propose a feasible alternative to PEGylation. This is not only relevant for OGBs, but can also be translated to other types of nanomedicines. As many therapeutics are administred intravenously, artificial cell membranes can be of large importance to the pharmaceutic industry.

3.3.3 PEG immunogenicity

As aforementioned, PEGylation has been considered the gold standard for surface modification of (nano)carriers. However, concerns about its biocompatibility have raised questions about the long-term safety of PEGylated therapeutics. An increasing amount of studies have shown that repeated intravenous delivery of PEGylated particles can induce an immune response. Anti-PEG antibodies were found in both animal and human patients, suggesting that the body does in fact recognize PEG as foreign, and generates antibodies against it [30, 41, 61]. This is especially concerning considering the discovery of ”pre-existing” anti-PEG antibodies in healthy volunteers who have never received PEGylated therapeutics. In 1984, Richter et al. conducted the first study on the prevalence of anti-PEG antibodies. They found anti-PEG IgM in 0.2% of healthy patients [53]. In 2016, Yang et al. analyzed 377 serum samples and 79 serum samples from the 1970s to 1990s. They detected both anti-PEG IgM and IgG, and found that up to 56% of the samples from the 1970s to 1990s contained anti-PEG antibodies. In 20% of the population IgG was detected, in 19% solely IgM, and 16% both IgG and IgM [69]. Yang et al. also found that in serum samples from 2016, 72% of the population contained anti-PEG antibodies. They hypothesized that the prevalence of pre-existing anti-PEG is increasing due to the excessive use of PEG in everyday products, such as food, household, and personal care products [69]. In cosmetics alone, more than 340 structures of PEG were used in 2015, as opposed to 7 structures in 1992 [20]. The increased prevalence of anti-PEG antibodies could mean that a first intravenous treatment with PEGylated therapeutics could cause an elevated immune response in part of the population, depending on the pre-existing anti-PEG titer.

The ABC phenomenon This elevated immune response to repeated exposure to PEG is referred to as the accelerated blood clearance (ABC) phenomenon. The ABC phenomenon affects the overall efficacy and safety of PEGylated therapeutics in the long term. Reduced circulation times and altered pharmacokinetics may lead to suboptimal drug delivery, limiting the effectiveness of the treatment. The ABC phenomenon is generated 4-7 days after the first exposure to PEG and gradually diminishes after about 3 weeks [30]. The mechanism behind the effect is that anti-PEG is formed after the first exposure. Anti-PEG IgM has a biological half-life of 3 weeks, but anti-PEG IgG can be present in the body for much longer. Upon the second exposure to PEGylated therapeutics, anti-PEG associates itself with the PEG chains on the surface of the therapeutic, which marks it for opsonization by complement proteins. This results in accelerated clearance of the particles and triggers an immune response. In some patients, PEG may cause a hypersensitivity reaction. Chang et al. found specific genetic defects that are significantly associated with high prevalence and concentrations of pre-existing anti-PEG in healthy individuals [8]. Hypersensitivity reactions are reported in many types of medications and can give mild to severe allergy symptoms after the first exposure, but more severe reactions after repeated exposure. This can result in anaphylaxis and even death. These types of reactions are also known as CARPA, as mentioned in section 3.3.1 [30, 41, 64]. CARPA was suspected in a group of patients who received the aforementioned Doxil® treatment. Approximately 10% of the patients experienced acute infusion-related reactions. After this, several studies investigated the interactions between Doxil® and anti-PEG antibodies in animal models. Elevated C3a levels were found after incubation with the anti-PEG antibodies, suggesting that CARPA can indeed be induced by PEG [20].

Currently, the exact mechanism of the immune response against PEG is still unknown. However, numerous studies show that PEG is not as biocompatible as previously thought. The discovery of

(pre-existing) anti-PEG antibodies suggests that the frequent usage of PEG in medicine will eventually lead to problems with immunogenicity and compromised therapeutic effects, if no alternate solutions are sought. Modifying the PEG moiety, the chain length, the degree of packing and/or the dosage schedule of PEGylated therapeutics can decrease the extent of the ABC phenomenon. But more importantly, alternative surface modification methods, such as lipid-based artifical cell membranes, should be explored to circumvent the limitations associated with PEGylation altogether.

3.3.4 ROS-induced cytotoxicity and antioxidants

The constructs in this thesis are based on CPO. OGBs based on peroxides release an intermediate product called H_2O_2. H_2O_2, as mentioned in section 3.2.3, is a member of ROS. ROS are highly reactive oxygen-containing byproducts of the oxygen metabolism and can cause oxidative stress-induced cytotoxicity in tissues when the levels are disturbed [51]. It is important to note that ROS do have a physiological function in the body, as some members of ROS play an important role in cell signaling [24, 52]. Although these mechanisms are not completely understood, it is evident that ROS interact with signaling molecules, such as MAP kinases in cell proliferation, and that ROS play a role in apoptosis and aging [52]. ROS can induce problems when oxidative stress occurs. Oxidative stress is an imbalance between ROS and antioxidants. Antioxidants neutralize or counteract free radicals. A shortage of antioxidants or an excess of ROS can cause a chain reaction in which free radicals steal electrons from other cellular components, which destabilizes them and generates more free radicals. This negative chain reaction can cause lipid, protein, and DNA damage. Consequences of this damage range from destruction of the cell membrane, to disruption of important cellular processes and prevention of cell division, to malfunctioning proteins [24]. This can be severe; ROS have been associated with multiple types of cancer, neurodegenerative diseases, metabolic and inflammatory diseases and vascular disease and heart failure [6]. Therefore, adequate antioxidant levels must be sustained in the body, to counteract the H_2O_2 that is released by the peroxides in OGBs. Because of this, several studies have incorporated antioxidants in their oxygen-generating constructs. Antioxidants break down H_2O_2 into water and oxygen, according to equation 2.

Multiple antioxidants can be included in OGBs for this purpose. Biological antioxidants, such as catalase, are enzymes that naturally occur in the body, where they fulfill antioxidizing processes. Catalase is present in all aerobic organisms. In humans, one of the places where catalase is found is in erythrocytes [58]. Catalase has been used in various types of oxygen therapeutics, from HBOCs and PFCs, to peroxide-based particles and hydrogels [1, 18, 44]. Since catalase is a naturally occurring antioxidant, it is biocompatible and the body can naturally break it down. However, the amount of ROS that the OGBs release and the amount of catalase that is incorporated in the constructs should be adjusted to each other. Just like an excess of H_2O_2, an excess of catalase can also disrupt ROS homeostasis. Regulating ROS homeostasis is extremely important when preventing cytotoxicity.

Superoxide dismutase (SOD) is another enzyme that is often used in OGBs. However, SOD catalyzes the conversion from the superoxide radical to O_2 or H_2O_2 [71]. Since the constructs in this research are based on CPO, they do not form superoxide. Therefore, SOD is not a suitable antioxidant for this research.

Some inorganic compounds can convert H_2O_2 to O_2. Since these materials do not naturally occur in the body to fulfill this purpose. Instead, they are inorganic compounds that have the capability of decomposing H_2O_2 into O_2. Most of these inorganic materials are not suitable for intravenous purposes, as they can not be broken down. However, manganese dioxide (MnO_2) is an inorganic catalyst that can be used *in-vivo*. After the reaction, MnO_2 will decompose to Mn^{2+}. Mn^{2+} is water

soluble, easily excreted, and naturally occurs in the body [72]. It is also a component of SOD, where it aids the antioxidation of ROS. Manganese plays an important role in regulating ammonia levels. Additionally, it aids the formation of hormones and plays roles in fat and carbohydrate metabolisms [14]. Since healthy manganese levels are very low, they might easily be disturbed when using MnO_2-based oxygen therapeutics. Alternations in the levels of manganese can be severe: An excess of manganese can lead to neurological damage. Manganese in the brain interferes with neurotransmitters and has been linked to Parkinson's Disease [14]. Neurotoxicity is the greatest concern of hypermanganesemia, though other biological processes can also be disrupted.

Because of the shortcomings of SOD and MnO_2, catalase was selected as the antioxidant in this research. Catalase is incorporated in the CPO-based OGBs with the goal of decreasing H_2O_2-induced cytotoxicity, increasing oxygen release, and for overall better biocompatibility and functionality of the constructs.

3.4 Conclusions

In this chapter, the urgency of oxygen therapeutics was described by highlighting the limitations of donor blood, which result in blood scarcity. Various types of oxygen therapeutics have been discussed, and the most promising candidate, SP-based OGBs, has been identified. The immune response to intravenously administered MPs has been briefly explained. This is crucial to understand, so the MPs can be designed in such a way that they induce a low immune response. For this, surface modification is necessary. Based on the information in this chapter, lipid-coated, catalase-containing, CPO-PCL microparticles are proposed as feasible RBC-substitutes. Both mentioned surface modifications, PEGylation and artificial lipid cell membranes, will be used to increase the hemocompatibility of the constructs.

4 Thesis outlook

4.1 Aim of the study

This research aspires to create a RBC substitute based on lipid-coated, catalase-containing, oxygen-generating PCL microparticles (LC-C-OG-PCL MPs). This main aim has been divided into several objectives, with corresponding research questions:

1) How can catalase be successfully incorporated in CPO-laden PCL MPs, and what is its effect on the release of H_2O_2 and O_2?

2) How can erythrocyte-inspired lipid coatings be employed to increase the hemocompatibility of catalase-containing OG-PCL MPs, and which formulation is the most hemocompatible?

3) Does the addition of a lipid coating affect the functionality of catalase and the release of H_2O_2 and O_2?

Catalase will be incorporated in the MPs in two ways, which will be described in Chapter 5. This incorporation will be assessed through various types of microscopy and by measuring the H_2O_2 and O_2 release of the MPs. It is hypothesized that the incorporation of catalase will catalyze the conversion of H_2O_2 into O_2, which decreases H_2O_2-induced cytotoxicity of the constructs. C-OG-PCL MPs are expected to release less H_2O_2 and to have an increased and more prolonged O_2 release than OG-PCL MPs. The addition of catalase to the MPs is thought to increase the surface roughness of the MPs, especially when added as an external coating on the MP.

For the second research question, two erythrocyte-inspired lipid formulations will be compared to each other and to uncoated MPs. A coating method for PCL was previously developed at our research group and this method will be used and adapted for C-OG-PCL MPs. One formulation (IT) is a close replicate of the biological erythrocyte membrane, and the other is a PEGylated analog (PT). The formulations will be discussed in more detail in Chapter 5. PEG is known to be immunosuppressive and is expected to be hemocompatible. However, if pre-existing anti-PEG is present in the blood, PEG can induce adverse effects. Because of this, artificial cell membranes are being researched as an alternative to PEG. To be regarded as a feasible alternative, the IT formulation should perform equal or better than PT in terms of hemocompatibility. In the presence of anti-PEG antibodies, the IT formulation is expected to be the most hemocompatible. The hemocompatibility of the different coated MPs will be assessed through a hemolysis assay, complement factor C5a activation, IgG activation, and a cell viability study. As anti-PEG is a type of IgG, if pre-existing anti-PEG is present, IT-MPs are hypothesized to include less IgG activation than PT-MPs. Both formulations are hypothesized to be more hemocompatible than uncoated MPs, due to their similarity to the erythrocyte membrane.

For the third research question, the elements from the first two objectives are combined. Lipid formulations are added to C-OG-PCL MPs and it is assessed if the addition of catalase and lipid coatings influences the release profiles, and how. It is not expected that the lipids disrupt catalase in any way, however, they will form an extra barrier. Therefore, the coatings might slow the release of the gases, but not decrease it, as cell membranes are permeable. The effect of the coatings on the release kinetics will be evaluated using H_2O_2 and O_2 measurements.

4.2 Thesis outlook

In this thesis, catalase-laden oxygen-generating MPs were developed. The aspired design of the MPs is discussed in Chapter 5. Two catalase-containing constructs were developed and compared

in terms of physicochemical characteristics and H_2O_2 and O_2 release profiles. The best-performing formulation was selected and further work was pursued using this specific formulation. All used techniques and assays are described in Chapter 6. The results section is divided per objective, and each section aims to answer the corresponding subquestion using the acquired data. The results and the position of this work with regard to relevant research are discussed in Chapter 8. Recommendations are given for future work. Finally, the research is compactly concluded in Chapter 9.

5 Microparticle design

Considering the aim and requirements for catalase-containing oxygen-therapeutics, as discussed in Chapter 3, the following chapter presents and discusses the design of the proposed constructs.

5.1 Different mechanisms of incorporating catalase

The MPs in this research generate oxygen based on the hydrolytic degradation of CPO. CPO is embedded in the hydrophobic polymer PCL, known for its biocompatibility, biodegradability, and hydrophobicity. This hydrophobicity makes it an excellent substrate for encapsulation of CPO, as it slows down the rate of hydrolysis. Catalase is included as an antioxidant. Two distinct catalase-containing formulations are proposed, and one formulation is chosen for further research.

1) **CI-OG-PCL MPs**: Catalase-incorporated OG-PCL MPs (**C**atalase **I**nside)

2) **CO-OG-PCL MPs**: Catalase-coated OG-PCL MPs (**C**atalase **O**utside)

The MPs are coated with different erythrocyte-mimicking lipid formulations. The exact composition of these coatings are discussed in section 5.2. A schematic overview of the MP designs is given in Fig. 3. Since PCL is a stiff and non-deformable polymer, the particles need to be smaller than erythrocytes to be able to safely maneuver through the capillary system without causing occlusions. Erythrocytes can deform and ”squeeze” through capillaries, with sizes ranging from 7.5-8.7 µm in diameter, and 2.2 µm as the maximum thickness of the disc [11]. The smallest capillaries have a diameter of 5 µm [12]. Without disrupting the flow of blood through these capillaries, the finalized particles will need to be below 5 µm.

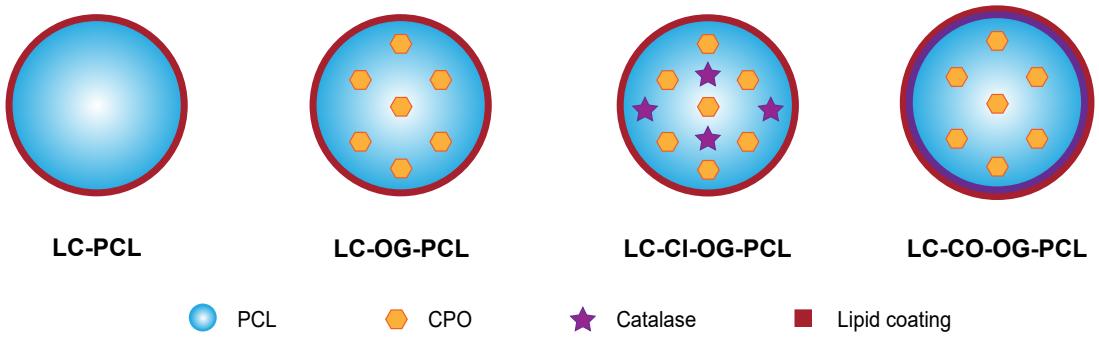

Figure 3 *A schematic overview of the different formulations of MPs.*

5.2 Erythrocyte-inspired lipid coatings

The MPs are coated with synthetic cell membranes, for which the biological RBC membrane serves as inspiration. The exoplasmic leaflet of the membrane, which is in direct contact with blood, determines the composition of the protein corona. It is important to understand the (dynamic) composition of the membrane, so it can be replicated.

The lipid bilayer of erythrocytes consists of cholesterol, sphingomyelins (SMs), and phosphatidylcholines (PCs). There is an asymmetry between the cytoplasmic and exoplasmic leaflet, and lipids can swap from the inside to the outside and vice versa. Cholesterol makes up about 30-40% of the membrane [35]. In erythrocytes, it is crucial that the cholesterol-to-phospholipid ratio is regulated. Lipid swapping and variations in the cholesterol percentage are related to multiple diseases, such as sickle cell disease, malaria, and atherosclerosis. Increased cholesterol content stiffens the membrane, which reduces deformability. It has also been

associated with delaying oxygen entry into the erythrocyte and slowing down oxygen release [7, 47]. The other 60-70% of the outer leaflet consists of phospholipids. Their distribution by molar percentage can be seen in Fig. 4. The phospholipids are asymmetrically distributed over the bilayer. PC and SM are mainly present in the outer leaflet. The amino phospholipids, phosphatidylethanolamine and phosphatidylserine (PS), are almost entirely found in the inner leaflet. Phosphatidylinositol (PI) is minorly found in the outer leaflet [36, 73].

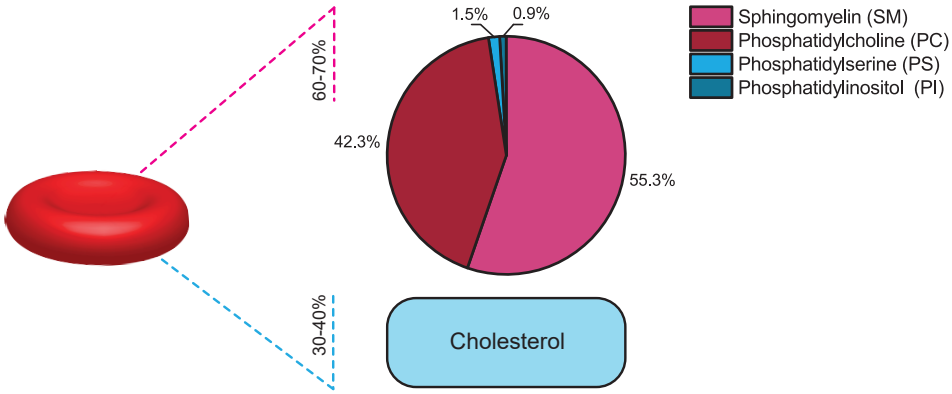

Figure 4 *The lipid composition of the exoplasmic leaflet of erythrocytes in molar percentages. Based on [35].*

Two erythrocyte-inspired lipid formulations were developed using synthetic analogs of the lipids in biological erythrocytes, such as cholesterol from ovine wool, egg SM, 1,2-dioleoyl-sn-glycero-3-phosphocholine (DOPC) for PC and SOY-PI for PI. The PI formulation is the closest replicate of the erythrocyte membrane, the PT formulation is a PEGylated variant of this formulation. Texas™-Red-DHPE is added to both formulations for visualization purposes, as it is a fluorescent lipid. The exact lipids compositions are found in Table 1.

Table 1 The lipid composition of the PI and PT lipid formulation.

	PI	**PT**
Lipid	*Molar percentage*	*Molar percentage*
Cholesterol	38.5	38.5
SM	34.9	34.9
DOPC	25.5	25.5
SOY-PI	1	0
DSPE-PEG-2000	0	1
Texas™-Red-DHPE	0.1	0.1

6 Materials and methods

6.1 Materials

All materials that were used in this research were acquired through the University of Twente. PCL (Average Mn 45,000), CPO powder, and catalase from bovine liver (2000-5000 units per mg protein) were supplied by Sigma-Aldrich, Germany. Lipids were acquired from Avanti Polar Lipids. Fluorophores, such as Amplex™ Red, Texas™ Red, and Alexa Fluor™ 488, were bought from Thermo Fisher Scientific, USA.

6.2 Methods

6.2.1 Microparticle production

MPs were prepared using a double emulsion (water-in-oil-in-water) method, similar to a protocol developed by Willemen et al. [66]. PCL was dissolved in dichloromethane (DCM) at 3% w/v to create the oil phase. The inner aqueous phase (AQ 1) varied depending on the MP type and could be ultra-pure water, henceforth referred to as Milli-Q water (MQ), CPO in MQ, or CPO and catalase in MQ. CPO was dissolved at 30 mg/ml with a total of 45mg, and 5 mg of catalase was added for CI-OG-PCLs. The mixture was sonicated by a tip-sonicator (25% amplitude, 1 min, 1s/1s pulse) on ice. The first emulsion was added to the second water phase, Mowiol 0.3%. Mowiol 0.3% is a surfactant and stabilizes the formed emulsions. The mixture was sonicated again (25% amplitude, 2 min, 1s/1s pulse). The mixture was stirred overnight at 600 RPM to evaporate the DCM. The following day, the MPs were washed 3 times with MQ and ethanol (2500*g*, 15 min, RT). Depending on the following experiments, the particles were redispersed in either isopropanol or MQ.

For CO-OG-PCL MPs, OG-PCL MPs were produced according to protocol. The particles were washed and redispersed in MQ. Catalase was added in excess (0.5mg/ml) and the mixture was placed on ice under slight agitation for 1 hour. Afterward, the MPs were washed with MQ to wash away any unassociated catalase.

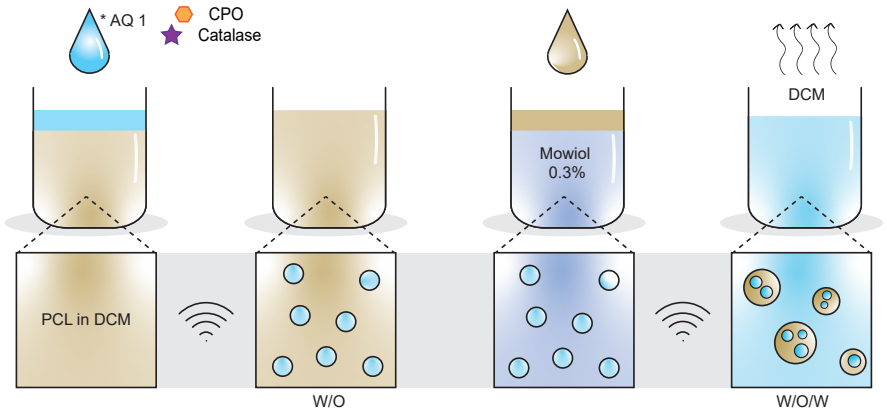

Figure 5 *(CI-OG)-PCL MPs can be made using a double emulsion method with Mowiol 0.3% as an emulsion stabilizer (schematic overview).*

6.2.2 Catalase-Alexa Fluor™ 488 conjugation

To assess the incorporation of catalase in CI-OG-PCL and to establish if the catalase-coating had formed properly on CO-OG-PCL, catalase was coupled to Alexa Fluor™ 488 succinimidyl ester. Catalase has accessible lysine residues, which served as sites for conjugation with the succinimidyl

ester. Catalase was dissolved in 0.1 M sodium bicarbonate buffer pH 8.3. The dye was dissolved in anhydrous DMSO and gradually added to the catalase solution whilst continuously stirring. The reaction was incubated for 1 hour at RT, protected from light. Finally, the solution was added to a Spectra/Por® Float-A-Lyzer, MWCO 8-10kDa, and dialyzed for 2 days on ice.

6.2.3 Lipid coatings

MPs were coated using an gradient-adapted Solvent-Assisted Lipid Bilayer (SALB) method for PCL MPs, based on works from Höhner and Ferhan [16, 22]. Lipid work solutions and MP in isopropanol were added together and a solvent-gradient was established by adding DPBS at a constant rate using a syringe pump. As the buffer concentration increased, lipids self-assembled on the MP surface, as seen in Fig. 6. The LC-MPs were heated in a water bath at 50°C for 45 minutes and washed 3 times in MQ (2500g, 15 min, 4°C).

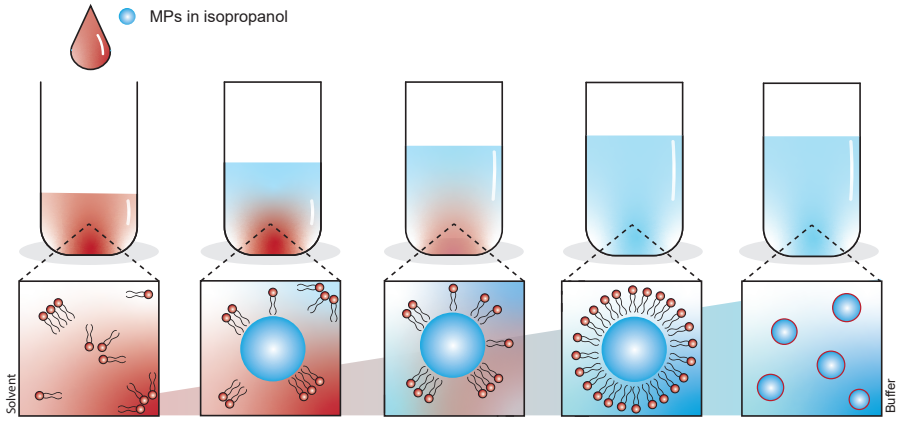

Figure 6 *Lipids self-assemble on the PCL surface using a gradient-adapted SALB protocol (schematic overview).*

For the coating of CO-OG-PCL, lipid film hydration was used instead of the adapted SALB protocol, to prevent the denaturing of catalase, as its optimum lies at 37°C [31]. A lipid cake was evaporated off the lipid work solutions under a nitrogen stream. CO-OG-PCL MPs were added in MQ. The emulsion was vortexed briefly to ensure thorough mixing of the lipids and MPs. LC-CO-OG-PCL MPs were washed once in MQ (3500g, 15 min, 4°C). The particles were analyzed using various types of microscopy. Lipid film hydration resulted in larger, multilamellar vesicles.

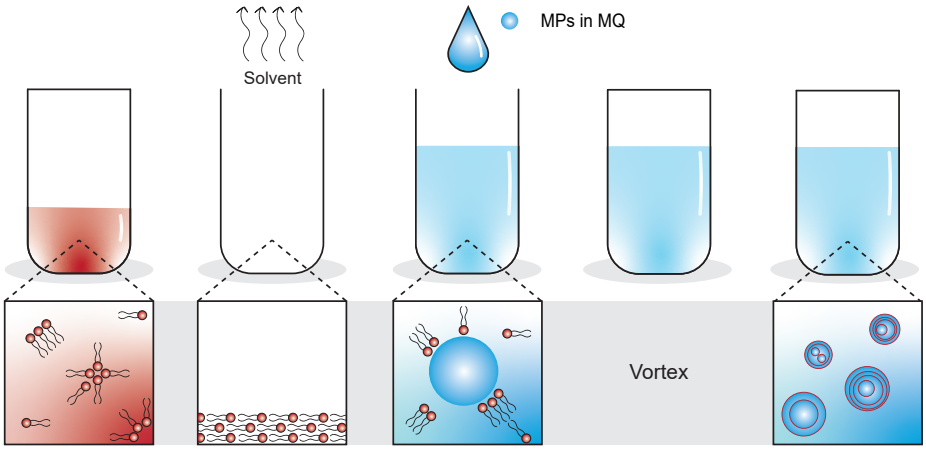

Figure 7 *Lipid film hydration is used to coat CO-OG-PCL, which creates giant multilamellar vesicles around the MPs (schematic overview).*

6.2.4 H_2O_2 release

The H_2O_2 release of the MPs was quantified using an Amplex™ Red assay (Thermo Fisher Scientific, USA). In the presence of horseradish peroxidase (HRP), Amplex™ Red is converted to resorufin. MPs in MQ were centrifuged and samples of the supernatant were taken at different time points and stored at -20°C until analysis. All of the supernatant was replaced with fresh MQ after each time point. The supernatants were placed in a 96-well plate with the working solution, consisting of HRP, reaction buffer, and Amplex™ Red. Resorufin was detected using a microplate reader (Varioskan™ LUX, Thermo Fisher Scientific, USA) with excitation 550 nm and emission 590 nm. The corresponding H_2O_2 concentration was calculated from the standards.

6.2.5 O_2 release

The O_2 release of the MPs was detected using two different types of oxygen sensors. In the earlier stages of this research, an optical oxygen sensor (Firesting-O2, Pyroscience GmbH, Germany) was employed to detect oxygen levels. Firesting-O2 detects oxygen-based based on the quenching of an emitted oxygen-sensitive indicator by the probe. The luminescence emission caused by the collision of the indicator and oxygen molecules is then detected again by the probe. The probe was pierced through the septum of a glass vial with MPs in DPBS. Oxygen release was measured for 2 to 3 days without stirring, under normoxic conditions. Because of limitations of the optical oxygen sensors, another sensor was employed for further measurements.

The measurements were continued with an electrochemical sensor, namely the Unisense UniAmp Single Channel System (Unisense, Denmark). Electrochemical oxygen measurements are based on measuring oxygen partial pressures. The detection is based on the diffusion of oxygen to an oxygen-reducing cathode, which is polarized against an internal Ag/AgCl anode. The experimental setup was similar to the previous setup. Highly concentrated MPs in MQ were transferred to a glass vial with a septum. The probe was pierced through the septum and the release was measured for 2 to 3 days. For the final measurements, the MPs were not stirred and were allowed to slowly deposit under normoxic conditions.

6.2.6 Hemolysis assay

Hemolysis is the rupturing of the erythrocyte membranes. If hemolysis occurs after incubation with the MPs, it indicates that the particles will damage native erythrocytes when in circulation. The hemolysis rate after incubation with MPs was determined through a hemolysis assay. Erythrocytes were isolated from whole blood, which was obtained through the Techmed Blood Donor Service. MPs were added to the isolated erythrocytes in DPBS in Eppendorfs. The samples were incubated for 4 hours on an orbital shaker at 37°C, 50 RPM. The samples were centrifuged at 300*g*, 5 min. The supernatant was added to a 96-well plate including positive (20% Triton-X) and negative (DPBS) controls. The absorbance was read in a microplate reader at 540 nm (Varioskan™ LUX, Thermo Fisher Scientific, USA). The hemolysis percentage (HP) was calculated using the following equation, where ABS+ is the mean absorbance of the positive controls and ABS- is the mean absorbance of the negative controls.

$$HP(\%) = \frac{(ABS_{\text{sample, RBC}}) - (ABS_{-})}{(ABS_{+}) - (ABS_{-})} \times 100 \tag{3}$$

6.2.7 C5a and IgG activation assays

The immunoactivation of the MPs was assessed by quantifying two whole-blood inflammatory markers: complement factor C5a and IgG. Complement factor C5a is released upon activation of the complement cascade and is associated with inflammation. IgG is an immunoglobulin, which

plays a crucial role in the adaptive immune response. IgG was chosen as a biomarker as anti-PEG is a type of IgG. Since all IgGs have the same constant domains and are distinguished by their variable domains, the constant domain is detected in this assay. Therefore, all kinds of IgG are detected, not just specifically anti-PEG IgG. The hypothesis behind this choice is that if IgG levels are higher after incubation with PT-MPs than with IT-MPs, some of these activated IgGs could be anti-PEG IgGs. This would mean that the blood sample contained pre-existing anti-PEG IgG. This is not unlikely, as mentioned in section 3.3.3. However, the titer of pre-existing anti-PEG should be sufficiently high.

For the whole blood incubations, freshly donated whole blood was obtained from the TechMed Donor Service. Immediately after withdrawal, Heparin 1.5U/ml was injected as an anticoagulant. The first tube was discarded, as this blood could contain more platelets, clotting factors, and contaminants as a result of the puncturing, and is not representative of the circulating blood. 500 µl of whole blood was incubated with 100 µl MPs and 100 µl CaMg DPBS at 37°C for 2 hours, under orbital shaking at 50 RPM in BioPur Eppendorfs. 50 µl EDTA 150 mM was added to each Eppendorf to stop the reaction. The tubes were centrifuged to separate the plasma from the erythrocytes at 1500*g* for 10 minutes and the plasma was then centrifuged again to separate the plasma from platelets (13000*g*, 10 minutes). The plasma was split into two and stored in Nunc Cryovials (one for each biomarker) at -80°C until further analysis.

C5a and IgG activation was determined using enzyme-linked immunosorbent assays (ELISAs). For C5a, a complement C5a Human ELISA kit was purchased from Thermo Fisher Scientific, USA. Lipopolysaccharides (LPS) were used as a positive control, which are known to activate the immune system. For IgG, a Human IgG ELISA Kit was purchased from the same supplier. LPS and Zymosan were used as positive controls. Zymosan induces inflammation by inducing pro-inflammatory cytokines. In both ELISAs, blanks served as negative controls.

6.2.8 Cell viability study

Cell viability after incubation with MPs was evaluated by a Live/Dead (Calceim AM/ethidium homodimer-1) and PrestoBlue™ assay. Human umbilical vein endothelial cells (HUVECs) were used as relevant cell type. HUVECs were ideally cultured until 80% confluency, but some areas of the flasks had lower confluency. The cells were trypsinized and transferred to a 96-well plate. The conditions were added and incubated with the cells for 24 hours. CPO 0.1 mg/ml functioned as a positive control. The negative control was EGM-2 medium. The MPs were resuspended in EGM-2 medium at roughly the same concentrations by comparing the size of pellets. However, the particle concentrations were not equal, which was noticed during the assay and which will be further discussed in the results. Per condition, 2 wells served for Live/Dead stains, and 3 wells were used for PrestoBlue™ analysis.

The Live/Dead wells were imaged using EVOS (EVOS Cell Imaging Systems, Thermo Fisher Scientific, USA), with a GFP channel for live cells and a Texas Red channel for dead cells. Transmission microscopy was used to visualize the particles. The images were analyzed using two Fiji (ImageJ) scripts. A script obtained from Allevi was used to count the live cells (Fig. 8A & B) [3]. Coated MPs contained Texas™ Red, which is imaged in the same channel as the ethidium homodimer-1 for dead cells. To distinguish between dead cells and MPs, the transmission image was overlaid with the thresholded Texas Red channel (Fig. 8C & D). Fluorescence that corresponded to MPs was deleted, so it could not be quantified by the script. This overlay also visualized the interaction between MPs and cells, and gave an idea of the MP concentration per condition.

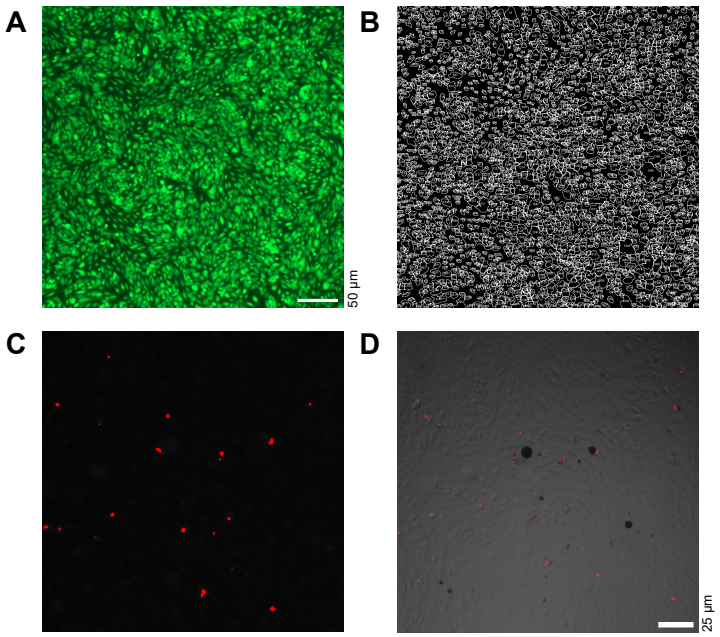

Figure 8 *Overview of the analysis of the acquired Live/Dead images using Fiji (ImageJ).* ***A*** *Live cells in the GFP channel* ***B*** *The counted live cells that the script identified* ***C*** *Threshold of the signal of dad cells and MPs in the Texas Red channel* ***D*** *The threshold merged with the transmission image to distinguish between dead cells and MPs.*

6.2.9 Statistical analysis

When possible, all experiments were performed using at least triplicates. Exceptions to this are the O_2 measurements, as the set-up only allowed to measure one sample per time. Poor reproducibility of the H_2O_2 and O_2 rendered the sample sizes too small, experiments from different dates could not be combined to create a larger population per condition due to bath-to-batch variability. This will be discussed in more detail in Chapter 8. Another exception is the Live/Dead assay, the assay was run in duplicates. When possible, data has been represented by mean ± standard deviation. Data was checked for normality using a Shapiro-Wilk test and when normally distributed, one-way ANOVA with post hoc Bonferroni test based on means comparison was used. When normal distribution could not be confirmed, a Kruskal-Wallis test with post hoc Mann-Whitney test based on median comparisons was used, as this test does not assume normal distribution.

7 Results

This chapter is divided into three sections. Each section corresponds to one of the research questions. The results aim to answer each question and a conclusion is given at the end of each section.

7.1 How can catalase be successfully incorporated with CPO-laden PCL MPs, and what is its effect on the release of H_2O_2 and O_2?

7.1.1 Size distribution and morphology

Morphology All MP formulations are depicted in Fig. 9A. Higher resolution imaging was acquired by scanning electron microscopy (SEM) (JSM7610F-Plus, JEOL Ltd., Japan). The incorporation of CPO and catalase into PCL was anticipated to result in increased surface roughness, based on a similar work [66]. This was barely observed. A batch of CO-OG-PCLs in which the catalase had not been properly washed after incubation, did show a layer of catalase covering the particles. Smaller clusters of catalase were found stuck to the MP. Energy dispersive X-ray spectroscopy (EDX) (Fig. 9C) was employed to detect calcium for CPO and nitrogen for catalase. No calcium was detected. Small amounts of nitrogen were detected, indicating that this layer is indeed catalase. A properly washed batch of CO-OG-PCLs did not show any trace of this layer, and no nitrogen was detected with EDX. CPO nor nitrogen was detected on CI-OG-PCL MPs either. The results suggest that the quantities of CPO and catalase were too low for proper detection using SEM/EDX.

Size distributions MP sizes were analyzed using optical microscopy (Nikon Optiphot, Nikon Corporation, Japan). Numerous images were captured per condition and analyzed in Fiji (ImageJ) by measuring the Feret diameter. The specific size distributions are given in Fig. 9D. A cut-off value of 5 μm was determined, as above this size, the MPs are not safe for intravenous delivery. The incorporation of CPO or CPO and catalase in AQ 1 (OG-PCL and CI-OG-PCL) did not increase the size range. The addition of a catalase coating (CO-OG-PCL) did seem to increase the sizes, as a larger percentage of the particles was above the cut-off value. However, this is likely due to aggregates of catalase with MPs, and not due to the individual MPs being larger.

Water contact angle In Fig. 9E, water contact angle (WCA) measurements of dried thick films of MP solutions do demonstrate differences between different MP formulations. Normality of the measurements was checked using a Shapiro-Wilk test, followed by a one-way ANOVA with post hoc Bonferroni test. OG-PCLs were more hydrophobic than PCL. This is unexpected, as PCL is a hydrophobic polymer, and CPO films had a WCA of 0°. This could be attributed to the formation of structures on the surface of the PCL as a result of the encapsulation of CPO. This is a phenomenon that was aspired to be observed on SEM, but was only minorly found. However, it is possible that these minor changes in surface chemistry, do result in an increased WCA. Since the CPO was not completely pure (75% purity), these other substances may be hydrophobic and have a higher tendency to go to the surface of the PCL. Another factor to consider is that OG-PCLs were more opaque in solution, and created films with more surface roughness. The relationship between surface roughness and wettability was described by Wenzel, who stated that increased surface roughness leads to enhanced wettability [65]. In the case of a hydrophobic material like PCL, that would lead to an even more hydrophobic WCA when measured on a rough surface [38, 65]. However, this was not observed, since neither PCL or OG-PCL had a hydrophobic WCA. What is possible, is that more air is trapped between the drop and the surface when the surface is rougher, increasing repellency. This could contribute to the larger contact angle.

The change in WCA between OG-PCL, CI-OG-PCL, and CO-OG-PCL suggests that low amounts of catalase are associated with the MPs. CO-OG-PCL MPs were completely hydrophobic, while CI-

OG-PCL MPs had an average WCA of 52.2°. The difference between the two catalase-containing formulations was statistically relevant. This demonstrates that the location of the catalase indeed differs. Based on confocal microscopy, it is known that the association efficiency of the catalase coating is low. Larger structures of catalase get surrounded by OG-PCL MPs, which was seen in Fig. 12. Since PCL as a material is hydrophobic, this suggests that catalase has its hydrophobic domains turned outwards, where PCL adheres.

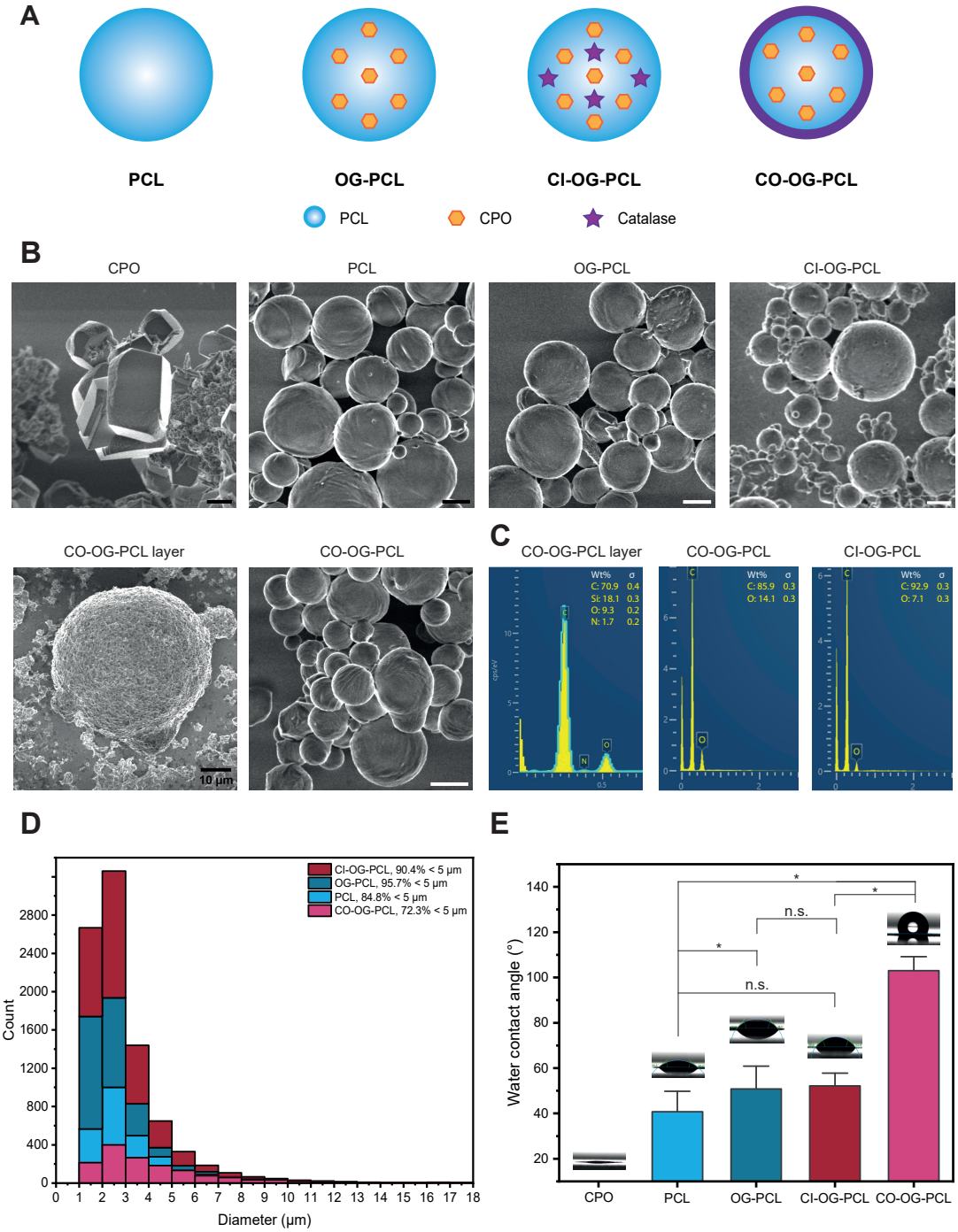

Figure 9 *Results regarding the morphology and size distributions of the MPs and CPO. **A** Schematic overview of the MPs. **B** SEM images of CPO crystals and MPs. Scale bars: 1 µm, unless stated otherwise. **C** EDX of CO-OG-PCL and CI-OG-PCL. **D** Size distribution of the different MPs. **E** Water contact angle measurements of the MPs. Significant differences are shown as *p < 0.05*

7.1.2 Addition of catalase in the inner aqueous phase can be used to create CI-OG-PCL MPs

CI-OG-PCLs were imaged by confocal microscopy. PCL was stained with Vybrant™ DiD Cell-Labeling Solution and catalase was linked to Alexa Fluor™ 488. Images were acquired and analyzed in ImageJ. Analyzed Z-stacks of CI-OG-PCL showed catalase at the same location as the OG-PCL MPs. It is thought that the catalase is located in the core of the MP, as it was added in the inner aqueous phase, but this is not confirmed. The catalase could be assembled on the surface of the particle. The Z-stacks do not give sufficient information to make this distinction.

7.1.3 Catalase and OG-PCL form aggregates upon incubation together

To create CO-OG-PCLs, catalase was incubated with OG-PCLs to form a coating on the surface. After incubation, the MPs were analyzed by confocal microscopy. PCL was labeled with Vybrant™ DiD Cell-Labeling Solution and catalase was conjugated to Alexa Fluor™ 488. The association efficiency of the incubation was low. Instead of catalase assembling on the surface of PCL, catalase forms aggregates in water, and OG-PCL MPs adhere to these structures. In some individual MPs, catalase was found on the surface.

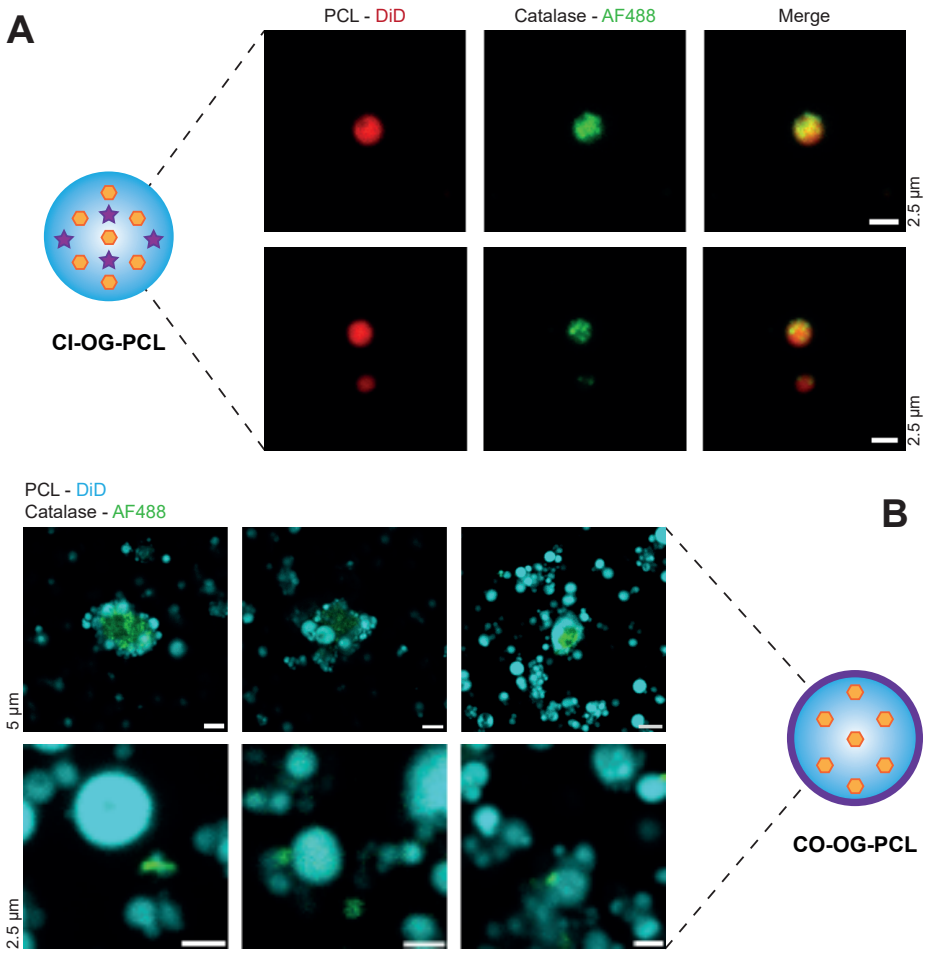

Figure 10 *Confocal microscopy of both formulations of catalase-containing OG-PCL MPs. **A** CI-OG-PCL MPs: Z-projections of the different channels at maximum intensity of all slices. **B** CO-OG-PCL MPs: Z-projections at maximum intensity of all slices. Top row: Catalase has aggregated and OG-PCL MPs assemble around it. Bottom row: Some individual MPs with catalase on the surface.*

7.1.4 Catalase lowers the overall H_2O_2 release of the MPs

The H_2O_2 and O_2 release of the MPs is shown in Fig. 11. The H_2O_2 release of pure CPO was characterized by a burst release within the first 5 hours (Fig. 11A). The release decreases and increases again, which is thought to be due to the outer layer of aggregates reacting first, subsequently exposing the inner CPOs. PCL MPs had a negative signal during the H_2O_2 measurements, which is likely due to autofluorescence of PCL residues in the supernatant, which interferes with the detection method (Fig. 11B). This will be discussed in more detail in Chapter 8. OG-PCLs were characterized by a similar burst release profile to CPOs (Fig. 11C). This suggests that some CPOs are encapsulated in the PCL, when comparing the difference to bare PCL. CI-OG-PCLs released less H_2O_2, but a burst within the first 5 hours was still observed (Fig. 11C). This might mean that catalase does break down H_2O_2, but not sufficiently to flatten out the initial burst. CO-OG-PCLs do not display this burst (Fig. 11C). The ”peak” of the release is delayed to 24-30 hours. This delay could be linked to the half-life of catalase, which is reported to be approximately 30 hours [40]. As a result of degradation, more H_2O_2 is released, until it naturally decreases when all CPOs have reacted.

The results displayed here are all individual measurements. Although measurements have been repeated, the reproducibility of the assay is low. Limitations of the H_2O_2 measurements will be discussed in Chapter 8 and supplemental data can be found in Appendix A.

7.1.5 OG-PCL MPs barely release oxygen

Oxygen release of the MPs was measured using two different methods. The results of the electrochemical oxygen measurements are given in Fig. 11D. CPOs had multiple bursts of O_2 release and over time, the release increased. This can be explained by the fact that the CPOs exist at various sizes, and once the outer layer of the larger aggregates has reacted, the CPOs on the inside are exposed to water and contribute to the second ”peak”. The results of the optical oxygen measurements are given in Fig. 11E & F. The measured burst by CPOs has similarities to the profile measured by the electrochemical oxygen sensor. Although PCL does not contain oxygen-generating elements, the signal drifted up over time. It is thought that the slow depositing of particles disturbs the signal. Data supporting this claim can be found in Chapter 8 and Appendix B. Another possible explanation is that the system was not completely air-tight. Two different formulations of OG-PCLs were measured. OG-PCLs fabricated with 45 mg and 60 mg of CPOs were used for the measurements. Oxygen release was detected, with a peak of 23.9% O_2 for OG-PCL 60. A similar slope of the release profile was observed for both OG-PCLs. The increase in CPOs did result in a higher oxygen payload and an extension from 29 hours to 46 hours of oxygen above physiological O_2%. Release profiles were only measured successfully once per condition.

Both sensors had problems regarding interaction of PCL with the detection method. This is discussed in more detail in section 8 and supplementary data supporting these claims can be seen in Appendix B & C. The electrochemical sensor also had a drift downwards. This was reported for all samples and the measurements were not stable in air. The manufacturer was contacted to verify if the sensor is malfunctioning, or if the measurements are not working well with the detection methods. The results from this sensor should be approached with caution.

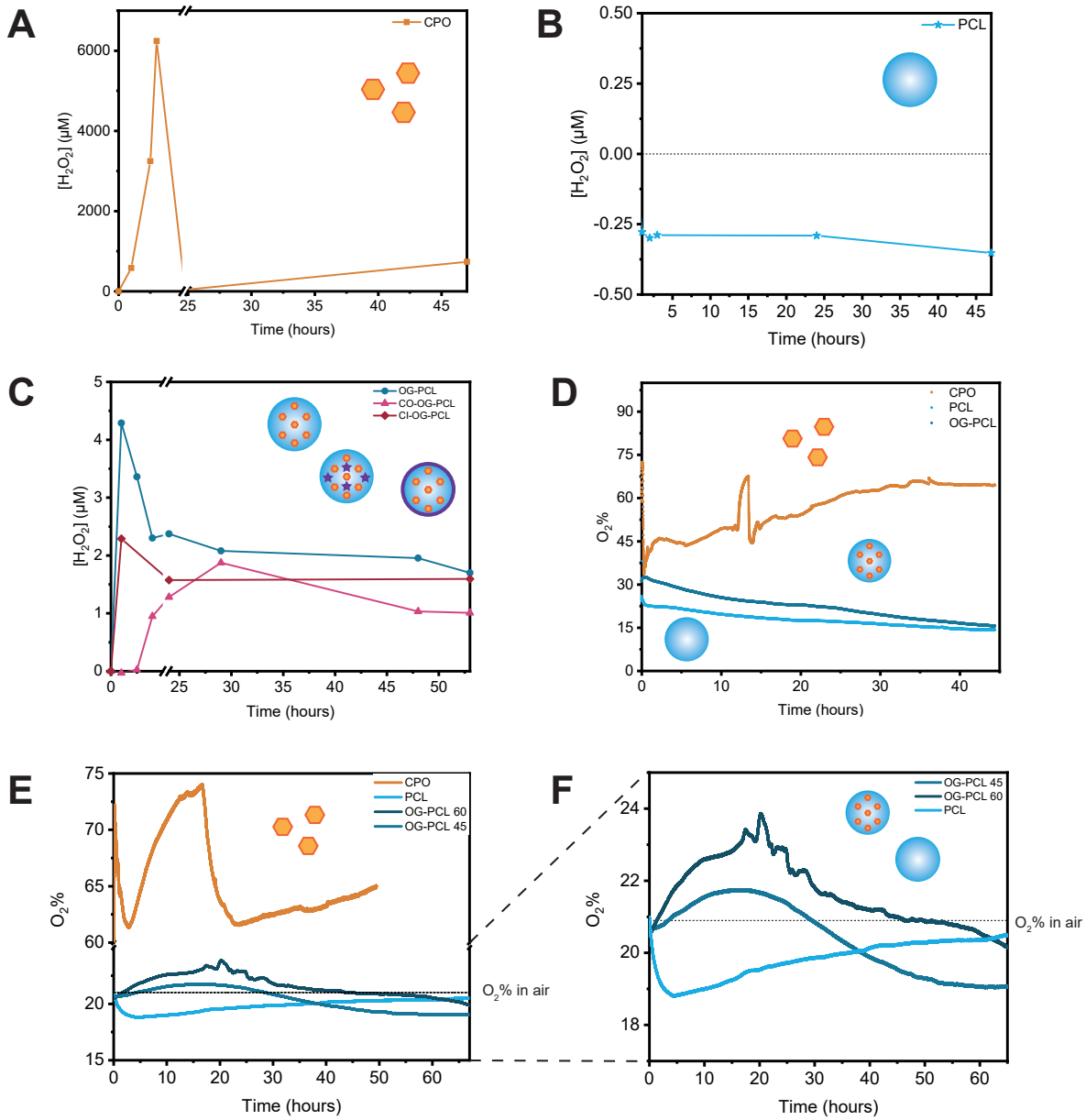

Figure 11 *H_2O_2 and O_2 release of the different MPs and CPO. **A** H_2O_2 release of CPO **B** H_2O_2 release of PCL MPs **C** H_2O_2 release of OG-PCL, CI-OG and CO-OG-PCL **D** Electrochemical O_2 measurements of CPO, PCL and OG-PCL **E** Optical O_2 measurements of CPO, PCL and 2 formulations of OG-PCLs **F** A close-up at the MP conditions of the O_2 measurements in E.*

7.1.6 Conclusions

Oxygen-generating PCL MPs can be fabricated using a double emulsion method, but there are limitations of the production process. The amount of CPO that was encapsulated in all oxygen-generating MPs was minor, and could not be detected using SEM or EDX. Indications that some CPO is encapsulated was found in the H_2O_2 assays and O_2 measurements. It was not possible to quantify the amount of CPO, however, it is evident that the amount is low. H_2O_2 release was detected for over 50 hours, optical oxygen measurements detected a maximum release of 3% of O_2 over the course of 46 hours.

Catalase-containing PCL MPs can be fabricated in two ways. The amount of catalase that is encapsulated in CI-OG-PCL MPs is too low to detect using SEM or EDX, however, catalase was visualized using a fluorescent probe and some catalytic capacity was measured during an H_2O_2 assay. This capacity was not sufficient to lower the cytotoxic initial burst of H_2O_2. For this reason, CO-OG-PCLs were selected as the catalase-containing formulation. An initial H_2O_2 burst was no longer observed. However, upon further analysis of the MPs, it was noticed that catalase was associated weakly with PCL, with most of the catalase being washed away by one simple washing step. The remaining catalase is mostly aggregated into larger structures, surrounded by OG-PCL MPs. It is thought that these larger aggregates of catalase contributed mostly to the decrease in H_2O_2. Some individual MPs with catalase on the surface remained after the washing, but the overall efficiency of CO-OG-PCL production is low.

7.2 How can erythrocyte-inspired lipid coatings be employed to increase the hemocompatibility of catalase-containing OG-PCL MPs, and which formulation is the most hemocompatible?

7.2.1 PCL and OG-PCL MPs can be coated with complex lipid formulations using the adapted SALB protocol

PCL and OG-PCLs were coated with an IT and PT lipid formulation using the modified SALB method. This method was developed to achieve stealthy, uniform layers around MPs. The coatings were imaged in a fluorescent microscope (Olympus IX71, Olympus Corporation, Japan). The coating efficiency was satisfactory and lipids seemed well-distributed over the MPs. Additional images of the established coatings can be found in Appendix D.

7.2.2 CO-OG-PCL can not be efficiently coated with complex lipid formulations

CO-OG-PCL MPs were coated with IT lipids using lipid film hydration. The coatings were evaluated using optical microscopy and confocal microscopy. Large multilamellar vesicles were seen on optical microscopy. The vesicles tended to fuse to larger aggregates of catalase and OG-PCLs. Based on the acquired images, the coating efficiency is low. There seemed to be an abundance of PCL compared to lipids. However, Vybrant™ DiD Cell-Labeling Solution is a stain that also stains lipids. Therefore, it is likely that some of the supposed PCL is lipids. Additionally, Texas™ Red's excitation lies at 586 nm, DiD at 649 nm. The spectra partly overlap, and therefore, some lipids were shown as cyan. This is thought to occur in the images in Fig. 12B-bottom. Vesicles are characterized by their "halo". These vesicles likely consist of lipids, as the PCL MPs are opaque, which was proven in samples without lipids. Texas™ Red-DHPE seems to be turned inwards and encapsulated by the other lipids. Another stain would have been more suitable to distinguish the difference between lipids and PCL.

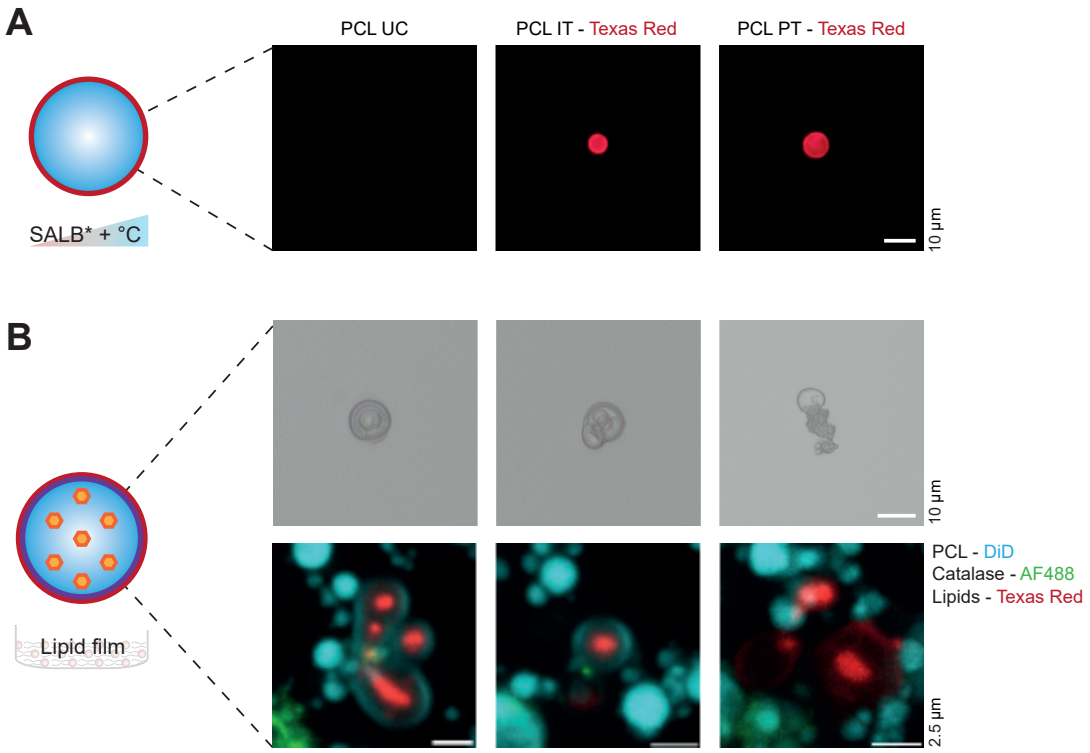

Figure 12 *Microscopy of the established coatings on PCL and CO-OG-PCL MPs.*
***A** Fluorescence microscopy of PCL MPs **B** IT-coated CO-OG-PCL MPs on optical microscopy (top) and confocal microscopy (bottom). Confocal images are Z-projections at maximum intensity of all slices.*

The lipid coatings have not formed well around the MPs, but rather, lipids are found in clusters and vesicles. This is due to the high melting temperature of SM. Both the IT and PT formulations require heating to form a uniform bilayer on PCL Above its melting temperature, SM becomes increasingly fluid. The lipids need to be in a liquid state to spread and adhere to the surface correctly. The heating also ensures that SM is evenly distributed through the lipid formulations. This is essential to achieve the right molar percentages of erythrocytes. Since catalase can't be heated to that extent, complex erythrocyte-mimicking lipid formulations containing SM are not suitable for this type of construct.

7.2.3 CO-OG-PCL can be coated with lipid formulations with lower melting temperatures

To demonstrate if catalase formed an obstruction for the lipid coatings to adhere, a new formulation without SM was introduced. This CT formulation consisted of 61.4% DOPC, 39.5% cholesterol from ovine wool, and 0.1% Texas™-Red-DHPE. CO-OG-PCLs were coated with the CT formulation using lipid film hydration, adapted SALB without heating, and adapted SALB with heating. PCL was stained with Vybrant™ DiO Cell-Labeling Solution (green). The results demonstrate that CT lipids do form well-established coatings on CO-OG-PCLs. Although fixed ratios of lipids to MPs were used, the coating efficiency of the adapted SALB method without heating was the highest. With lipid film hydration, lipids ended up in larger vesicles, and many particles remained uncoated. The adapted SALB method with subsequent heating showed a low MP concentration and giant aggregates of particles with supposedly catalase. The sample was visibly aggregated to the naked eye. It is thought that catalase is denatured during the heating step, and this denaturation results in this aggregation. To conclude, when using the adapted SALB protocol without subsequent heating, CO-OG-PCL MPs can be coated in a satisfactory way.

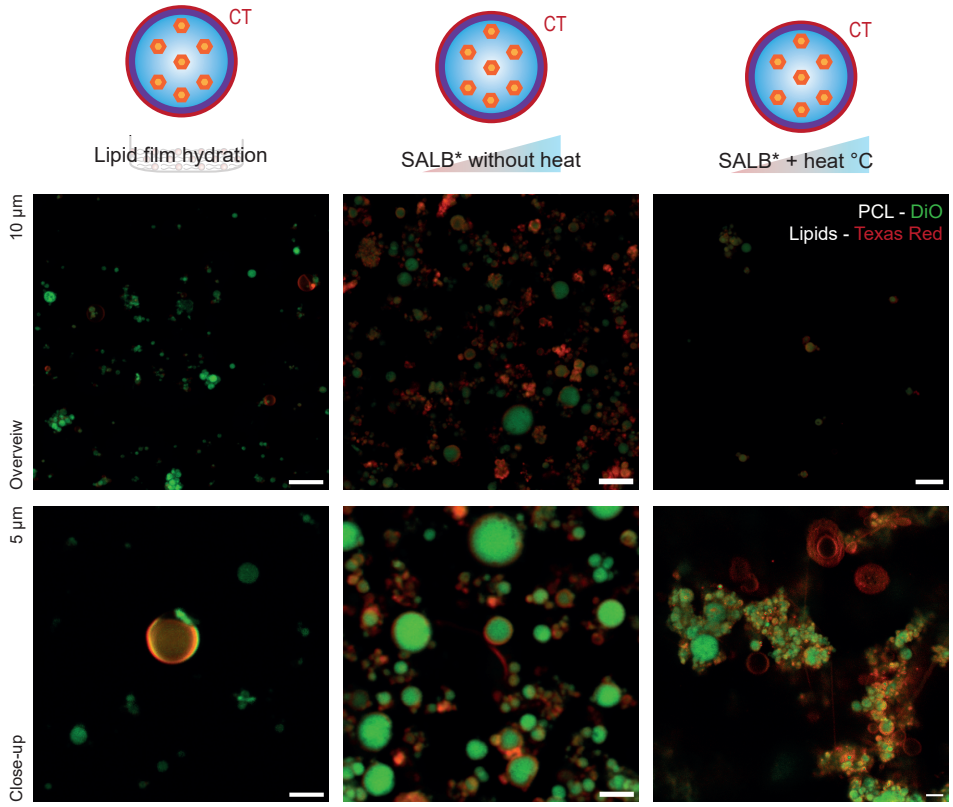

Figure 13 *CO-OG-PCL MPs can be coated with the CT formulation using 3 different methods. Confocal microscopy of CT-CO-OG-PCLs, coated by lipid film hydration, adapted SALB without heating and adapted SALB with heating.*

7.2.4 IT-PCL MPs have the lowest hemolytic rate

All PCL samples showed low hemolytic rates (Fig. 14). The ASTM standard F756-00 classifies biomaterials as non-hemolytic (0–2% hemolysis), slightly hemolytic (2–5% hemolysis), and hemolytic (>5% hemolysis) [13]. Using these values, uncoated PCL and PT-PCL are slightly hemolytic and IT-PCL is non-hemolytic. However, the differences were not statistically relevant.

7.2.5 CO-OG-PCL MPs induce less C5a and IgG activation than PCL MPs

C5a activation assay Fig. 14C shows the mean C5a activation per condition. The data was checked for normality using a Shapiro-Wilk test. LPS and CO-OG-PCL PT were not drawn from a normally distributed population. Therefore, a non-parametric Kruskal-Wallis with post hoc Mann-Whitney test was conducted at a significance level of p=0.0024. No significant differences were found between the samples. Nevertheless, both PCL and CO-OG-PCL MPs exhibited higher C5a activation levels when coated with the IT formulation, compared to PT and uncoated MPs, although not statistically relevant. CO-OG-PCL MPs induced slightly lower C5a levels than PCL MPs, suggesting that CO-OG-PCLs are more hemocompatible. This is thought to be due to the catalase, which reduces interactions of the particles with whole blood markers such as C5a. Various conditions induced more C5a production than LPS. Therefore, LPS was not a suitable positive control for C5a. Zymosan would have been a more appropriate positive control.

IgG activation assay The results of the IgG activation assay are given in Fig. 14D. All variants of CO-OG-PCL MPs induced significantly less IgG activation than uncoated PCL. The catalase appears to have a hemoprotective effect on the MPs, possibly by altering the surface chemistry of the MP and reducing interactions with IgG. Uncoated PCL performed similarly to the positive controls, indicating its high immunoactivity for IgG. For IgG activation, the PT formulation induces the lowest immune response. Since a general IgG ELISA kit was used, all kinds of IgGs were activated by this assay. It is not possible to draw a specific conclusion for anti-PEG IgG. It is not known if any anti-PEG was present in the blood and activated by this assay. It is difficult to say which specific immune response is activated after incubation with each condition. However, higher IgG levels do suggest that the immune system is actively recognizing and responding to the MPs, as IgGs are produced in response to foreign objects or pathogens.

The C5a and IgG activations per condition per donor are given in Appendix E. Donor 2 induced higher C5a levels, but with a larger standard deviation. It is not unlikely that donors react differently to the MPs, however, that would not account for the larger error margins. It is possible that some of the ELISA strips used for this donor were damaged during the washing steps. There were not any remarkable differences between donors for IgG activation.

7.2.6 Cell viability

The cell metabolism of HUVECs after 24-hour incubation with MPs was assessed through Live/Dead analysis and a PrestoBlue™ assay. The results are given in Fig. 14E & F. Supplemental data can be found in Fig. 15 at the end of this section. CPOs were used as a positive control and induced cell death in the vast majority of the cells. All cells that were exposed to MPs had cell viabilities above 80%, rendering the MPs non-cytotoxic according to ISO 10993-5 [25]. Coated CO-OG-PCLs seemed to disintegrate in the medium, this was observed by many fragments of particles. On the other hand, larger aggregates were also found. It is possible that the particles aggregated after shredding their lipid coatings, as the PCL aggregates in aqueous medium. The sizes and the amount of the particles, aggregates and fragments were counted in Fig. 15B & C. Although no cell death was observed as a result, the MPs were damaged and could no longer fulfill their purpose. The lipid coatings seemed to be shredded. This is in line with results from section

7.2, where it was established that IT and PT formulations could not form stable coatings on CO-OG-PCLs. The largest amounts and sizes of aggregates were found in wells that were exposed to IT-CO-OG-PCL. These cells had the lowest cell viability based on both the Live/Dead and the PrestoBlue™ assay, indicating that the MP disintegration does induce cell death to some degree. It is important to note that the HUVECs in this study were on passage 6. The HUVECs could have been quite resistant.

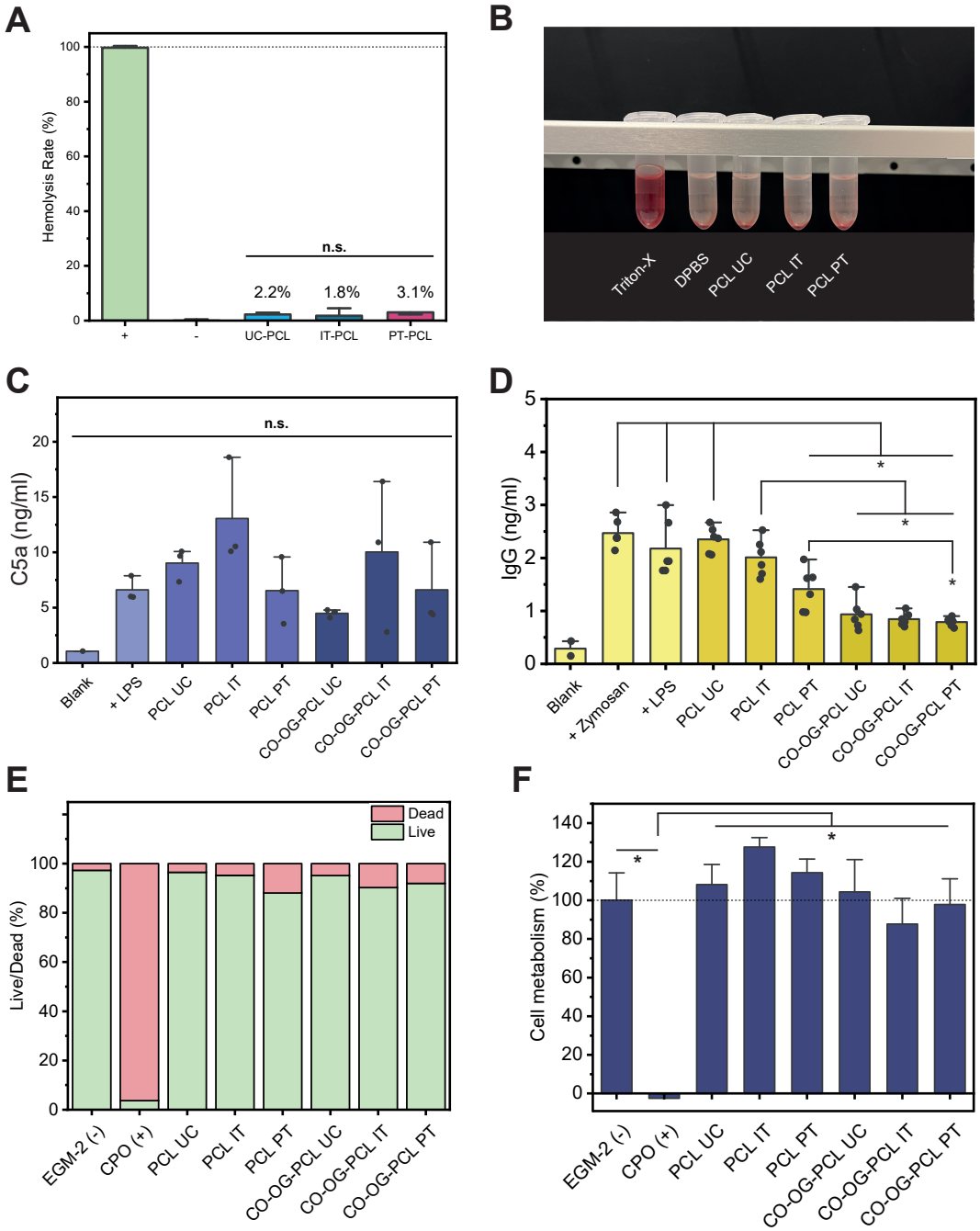

Figure 14 *Results from all the hemocompatibility studies.*
***A** Mean hemolytic rates (%) of the samples. Hemolytic rates were determined using one donated blood sample and 5 replicates per condition. **B** Pellets of the conditions after incubation with RBCs. **C** C5a activation per condition, all donors combined. No statistical differences were found. **D** IgG activation per condition, all donors combined. Significant differences are shown as *p < 0.05. **D** Cell viability per condition based on the Live/Dead assay. **E** Cell metabolism per condition based on a PrestoBlue™ assay. Significant differences are shown as *p < 0.05*

7.2.7 Conclusions

Lipid coatings PCL and OG-PCL MPs can be successfully coated with the complex erythrocyte-inspired lipid formulations IT and PT. The coatings were stable in aqueous solution and medium. It was not possible to coat CO-OG-PCL MPs with complex lipid formulations

containing SM, because catalase denatured when subjected to heating above 37°C. Heating is necessary for lipids with higher melting temperatures, like SM, to phase-transition. CO-OG-PCLs can be coated with CT lipids, consisting of cholesterol and DOPC. The modified SALB method without subsequent heating displayed a high coating efficiency and uniform coatings on MP surfaces. Few aggregates were found, indicating that the coatings inhibit MP aggregation. This is desired. Therefore, with the introduction of the CT formulation, an efficient way of coating CO-OG-PCL MPs was found.

Hemocompatibility of the MPs MP hemocompatibility was assessed using a variety of assays. All variants of PCL MPs induced rarely any hemolysis. PT-MPs were associated with lower C5a and IgG levels for both PCL and CO-OG-PCL. PEGylation indeed lowers the complement and overall immunoactivation caused by MPs, which is in line with literature and with approved formulations and therapies.

CO-OG-PCL MPs induced a less pronounced immune response than PCL MPs. The catalase ensures that less H_2O_2 is released, which reduces the cytotoxicity of the MPs. Catalase also reduces the interactions of the MPs with immunoactive elements such as C5a and IgG. It is important to note that the coatings in these studies were not well-formed on the surface of the MPs. In cell culturing medium, the MPs disintegrated and the lipids seemed to be shredded. Although cell viability was still high after incubation, MP disintegration is not desirable. Moreover, the HUVECs in this work were on the 6th passage at the time of incubation and were seeded with low confluency. As a result, they might have been more resistant than cells of earlier passage.

To conclude this research question, CO-OG-PCL MPs can not be properly coated with SM-containing lipid coatings without heat. Unstable lipid vesicles formed around CO-OG-PCL MPs when coated with complex lipid formulations using a film hydration method. Remarkably, these coatings did give good results during hemocompatibility studies. This is presumably partly contributed to the addition of catalase in the MP, which reduces the cytotoxicity by breaking down H_2O_2 that is generated by the CPOs. It also may reduce the interactions of the MP with immune factors in the plasma, such as C5a and IgG. Between the IT and PT lipid formulations, PT-coatings were overall more hemocompatible. As these complex lipid formulations could not be used on CO-OG-PCL due to melting temperatures above the optimum of catalase, a CT formulation was introduced, which did not require any heating. It is recommended to repeat the hemocompatibility studies with the CT formulation, as this coating is stable and showed high coating efficiencies on CO-OG-PCLs.

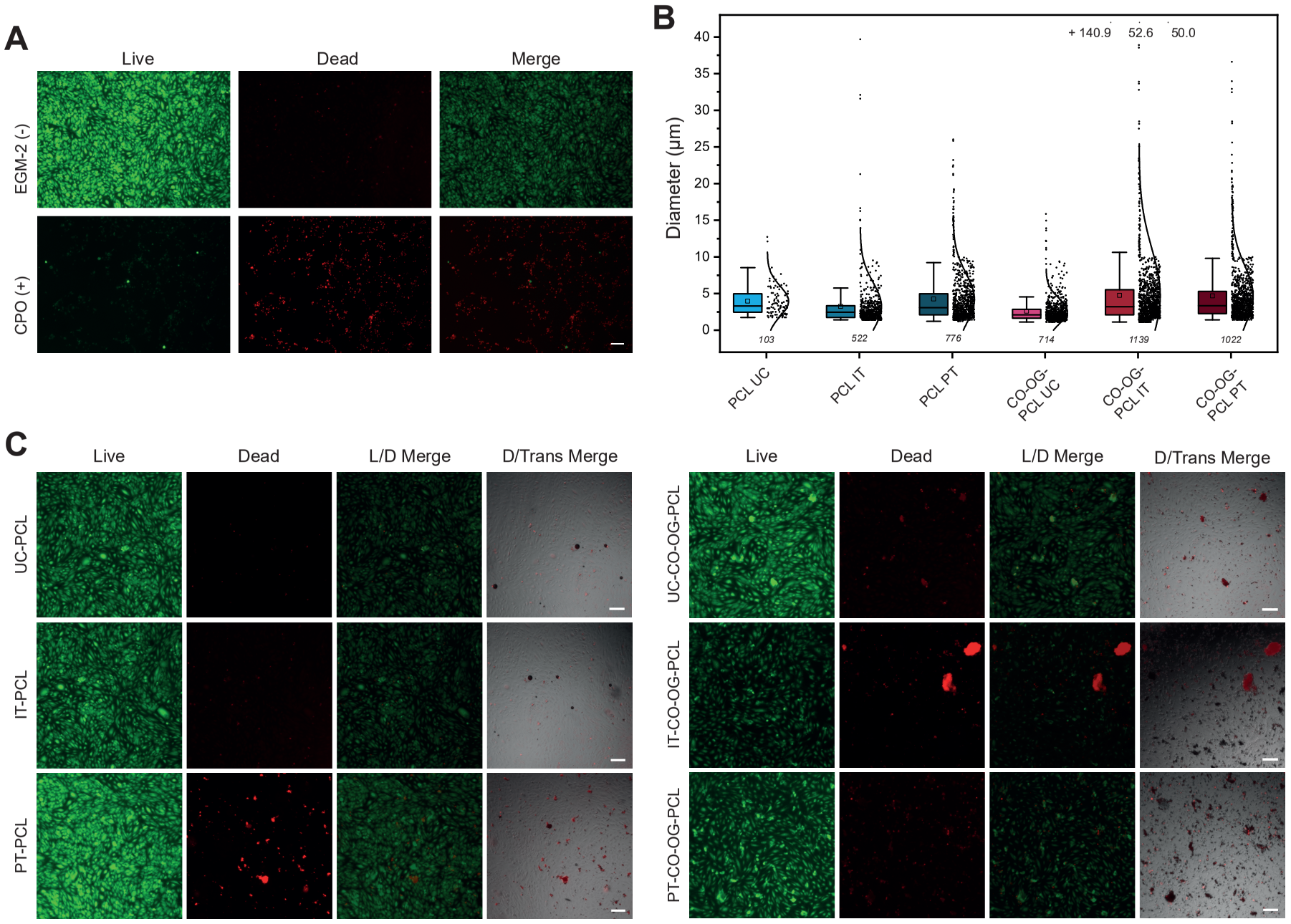

Figure 15 *Additional data and microscopy of the Live/Dead assays.* ***A*** *Live/Dead images of the positive and negative controls.* ***B*** *The number of particles, aggregates and fragmentations combined per condition and their respective sizes.* ***C*** *Live/Dead images of the wells that were exposed to MPs. A merge of the transmission image and the dead image is included, so signal from particles could be excluded and the interaction between cells and particles could be observed.*

7.3 How does the addition of a lipid coating affect the functionality of catalase and the release of H_2O_2 and O_2?

At this point of research, the CT lipid formulation was not yet established. Therefore, the IT formulation was used to answer this question. At that point, the IT formulation was the most interesting to evaluate, as it proposed an alternative to PEGylation, which is still an interesting line of research regarding PEG immunogenicity.

7.3.1 Lipid coatings slightly lower the H_2O_2 release of MPs, but do not affect the catalyzing capacity of catalase

The effect of the lipid coatings on the H_2O_2 release was assessed with an Amplex™ Red assay. It was especially important to investigate whether the coatings disrupted the functionality of catalase. The release profiles are plotted in Fig. 16 and clearly show that the lipid coatings are permeable to H_2O_2. Noticeably, less H_2O_2 is released when compared to uncoated MPs. The lipid coatings may slow down the release of H_2O_2, as they form a barrier. The functionality of catalase was not disrupted by the addition of a lipid membrane. IT-CO-OG-PCLs still display the catalyzing effect of catalase.

There are some limitations and problems that were faced during the H_2O_2 studies, mainly regarding the low reproducibility of the measurements. These will be discussed in Chapter 8. Supplementary data can be found in Appendix A.

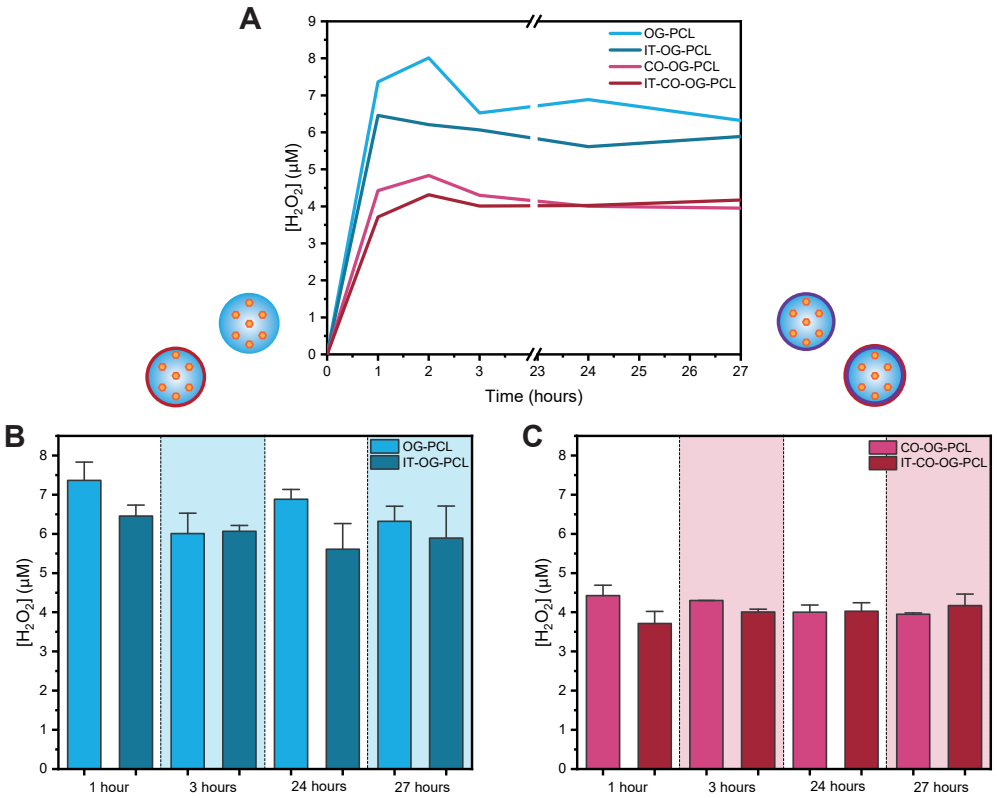

Figure 16 *The H_2O_2 release profiles of lipid-coated OG-PCLs and CO-OG-PCLS.* ***A*** *H_2O_2 release profiles of coated and uncoated OG-PCLs and CO-OG-PCLs.* ***B*** *Bar chart of the H_2O_2 release of OG-PCL and IT-OG-PCL. The addition of the lipid membrane slightly reduced the release.* ***C*** *Bar chart of the H_2O_2 release of CO-OG-PCL and IT-CO-OG-PCL. The addition of the lipid membrane barely reduced the release.*

7.3.2 Conclusions

The addition of a lipid coating does not seem to affect the functionality of catalase. CO-OG-PCLs with and without lipids released less H_2O_2 than similar OG-PCLs, displaying catalytic capacities. However, based on earlier results, it is known that IT lipids do not form well-established coatings around CO-OG-PCLs. Part of the MPs remains uncoated after lipid film hydration, and agglomerates of catalase, OG-PCL and lipid vesicles were likely present in the samples. These agglomerates might overshadow the results of individual particles. It is recommended to repeat these studies using CT-coated CO-OG-PCLs.

O_2 measurements were not feasible on coated MPs. The yield of the developed coating methods is low, and both oxygen detection methods were not sufficiently sensitive to detect oxygen from small amounts of particles. Shortcomings of the oxygen measurements are discussed in further detail in Chapter 8.

8 Discussion

In this chapter, the overall MP design and the obtained results are discussed. Limitations are identified and recommendations for better detection methods are given. Finally, the position of this work compared to other research in the field is discussed and concrete recommendations for further work are proposed.

8.1 Limitations of the OG-PCL MP design

A large limitation of the proposed oxygen-generating constructs and the production process of the constructs is that barely any CPOs were able to be encapsulated. This reduced the oxygen-generating potential to non-clinically relevant levels. The encapsulation mechanism is not understood, and despite many attempts, the encapsulation of CPOs could not be proven. Indications that trace amounts of CPOs were associated with the MPs were identified through H_2O_2 and O_2 release studies, but the detected concentrations were low. The aim to produce PCL MPs below 5 μm has made encapsulation near impossible, as CPOs are not stable at micrometer sizes. Therefore, the clusters of CPOs may simply be too big to be incorporated in the MPs. Furthermore, despite PCL being regarded as biocompatible, uncoated MPs visibly flocculated and formed aggregates over time in an aqueous medium. This would propose a problem *in-vivo*, as this is not safe for intravenous delivery. Hemocompatibility of uncoated particles was lower than coated particles, highlighting the need to coat the particles. This is possible, but the addition of catalase complexities this process. This will be discussed in section 8.1.3.

8.1.1 Limitations of the H_2O_2 release studies

Since there was no control over the encapsulation of CPOs, batch-to-batch variety and poor reproducibility of measurements was an issue. All batches that were analyzed generated H_2O_2, but, it is very hard to state how much H_2O_2 each condition releases. A pattern can be distinguished, which showed that in multiple batches, CO-OG-PCLs did generate less H_2O_2 than OG-PCLs. It is based on these types of patterns that it is stated that CO-OG-PCLs and CI-OG-PCLs release less H_2O_2 than OG-PCLs. It is important to consider that these statements are not statistically proven. An enzymatic assay, like Amplex™ Red, might not be the most suitable method for detecting H_2O_2 at these concentrations, as enzymatic assays have limited sensitivity, which was an issue when detecting H_2O_2 from lipid-coated OG-PCLs and CO-OG-PCLs. Various measurements failed, as the detected amounts were too low to fit right to the established standard curves. Both inter and intra-variability was an issue with detecting the release from coated MPs. Additionally, PCL itself is slightly autofluorescent, which introduces a factor of uncertainty within the measurements [49]. According to Qi et al., PCL is mainly autofluorescent in the FITC channel (475 to 650 nm) [49]. The fluorescence of resorufin in the Amplex™ Red assay is measured at 530 nm excitation and 590 nm emission. Therefore, signal can be disturbed by the autofluorescence of PCL. A feasible alternative to enzymatic quantification of the H_2O_2 release is through scavenging assays. The MPs would be dispersed in a known, higher concentration of H_2O_2. The amounts and rate at which catalase decomposes H_2O_2 can be quantified by measuring the concentration over time. Higher amounts of H_2O_2 are a lot more stable and can be detected through various mechanisms. Electrochemical probes and High Performing Liquid Chromatography can be used to quantify the amount of H_2O_2 after exposure to MPs after separation from the MPs [60]. Supplemental data supporting these claims regarding the limitations of the H_2O_2 studies can be found in Appendix A.

8.1.2 Limitations of the O_2 release studies

Batch-to-batch variability was also a problem during O_2 studies, as the amount of CPO determines the oxygen-generating potential of the particles. What makes the O_2 studies even more

complicated is that PCL seemed to interact with both detection methods. Changes in stirring or depositing of particles induced changes in the measurements. This was observed for both the optical and electrochemical measurements, which is shown in Appendix B and C. The optical oxygen measurements are based on the quenching of an emitted oxygen-sensitive indicator by the collision of oxygen molecules with the indicator. The interaction between PCL and the indicator might disrupt this principle. Additionally, PCL might scatter the signal. Despite this, minor oxygen release was detected for two variants of OG-PCL with different amounts of CPO. Due to the limitations mentioned here, there is a degree of uncertainty in these measurements. The optical oxygen system was also not very sensitive, large amounts of particles had to be used, up to the whole batch. The detection method was not sensitive enough to detect oxygen from smaller amounts of particles nor detect the effect of catalase. When compared to other works, the detected amount of oxygen is marginal. Therefore, some trial measurements were conducted under a nitrogen atmosphere. This set a low baseline and would make the increase in oxygen easier to measure. However, this was in practice not possible, as the system was not 100% air-tight, and the increase in oxygen could be partially due to air getting in the system. This can be seen in the release of PCL in Fig. 11, where the release of PCL drifts up. Another limitation with placing vials under nitrogen atmosphere was that the O_2% was never at 0% and never the same between batches. Since physiological air is at a constant O_2%, it was decided to measure the particles in physiological O_2%. The incentive was that this would make it easier to compare the different samples. For the optical oxygen sensor, this approach was used to compare the conditions in Fig. 11.

With the electrochemical sensor, it is suspected that calibration and drift issues of the probe caused that the measurements didn't stabilize. The start values of some of the samples were around 30% of oxygen, which was not reliable. This is thought to be due to wrongful calibration, as the measurements did not stabilize for setting the value of oxygen in air, nor in 0% solution. The manufacturer has been contacted to verify if this is a malfunctioning of the probe. At this point, the electrochemical sensor could not provide any valuable and trustworthy information regarding the oxygen releases. Interestingly, the release of CPOs with optical and electrochemical oxygen sensors was very similar. The pattern of the release measured with the electrochemical oxygen sensor is probably right, as the CPOs did not interact with the probe, but the calibration is still unsure.

A limitation with the nature of the O_2 and H_2O_2 measurements is that the release could only be measured 24 hours after production, due to evaporation of DCM and due to the washing steps. In these first 24 hours, both gases are generated, likely in larger concentrations than detected after 24 hours. Therefore, the finalized particles should release oxygen for long after 24 hours for it to be clinically relevant. When upscaling, the production process can likely be optimized and sped up. However, the particles would have to be produced, sterilized, and transported to hospitals for transfusions. Once transfused, they have to retain the capacity to release more oxygen for multiple days. The oxygen release that was detected on OG-PCL 60 lasted for 46 hours. This is not prolonged enough to be clinically relevant. Based on the literature, alternatives for oxygen detection are given. Many studies have successfully created OGBs, based on CPO with other substrates as encapsulation materials. Oxygen release was detected by producing the OGBs and measuring the release in hypoxia chambers or by using more sensitive equipment, like blood gas analyzers [23, 50].

8.1.3 The incorporation of catalase limits the complexity of the lipid coatings

Catalase could be encapsulated in CI-OG-PCLs, but, like CPOs, only trace amounts were encapsulated. At this point in the research, CO-OG-PCLs seemed a better candidate as they managed to flatten out the burst release of H_2O_2. After conjugation to a fluorophore, it became evident that the association efficiency of catalase to PCL is low, and catalase formed aggregates in water. The association with OG-PCL MPs was weak, the catalase layer that was seen on SEM was washed away when purifying the solutions from unassociated catalase. Encapsulation of catalase is

a more stealthy method of producing catalase-containing MPs, as no aggregations can be formed and the catalase cannot be washed away. It is worth investigating if in larger PCL MPs, catalase can be encapsulated at higher concentrations.

The addition of catalase limits the complexity of suitable lipid coatings. Catalase denatures when heated above its optimum temperature. A simplified erythrocyte-inspired coating based on cholesterol and DOPC did form well-established, uniform coatings around CO-OG-PCLs when using the adapted SALB protocol without heating. Based on confocal microscopy, the yield and coating efficiency were satisfactory. On Z-stacks of particles, it was seen that the coatings were present of almost all the analyzed particles, and the fluorescence was evenly spread on the surfaces. It is encouraged to continue work with this lipid formulation and to investigate if the limited complexity of the formulation induces issues with hemocompatibility.

Despite issues with the formation of the catalase layer and complex lipid coatings, CO-OG-PCLs performed better than all formulations of PCL during hemocompatibility studies. Cells were viable after exposure to the particles, even after particle disintegration and lipid shredding, however, it is important to consider that the cells that were used during this study were possibly quite resistant. Of the two complex coatings, PT was associated with the best hemocompatibility overall, highlighting the immunoprotective capacities of PEG. It is worth investigating if a second exposure to the PEGylated constructs induces higher C5a and IgG levels, as this would suggest that anti-PEG immunogenicity is occurring. A PEGylated-CT formulation can also be introduced, to continue the evaluation of whether a bio-inspired coating is a feasible alternative to PEGylated coatings for CO-OG-PCLs.

8.1.4 Statistical analysis

Because of the large batch-to-batch variability, sensitivity issues of the measurements, and because of the set-up of certain experiments, statistical analysis is not very strong. Sample sizes per condition were not large enough for the H_2O_2 and O_2 measurements. As the oxygen set-ups only had one probe available, only one sample per batch could be measured. Different batches were not comparable and many batches were unreliable due to the limitations of the detection methods, for both H_2O_2 and O_2 measurements. It is highly recommended to use more sensitive detection methods and more probes, so the same batch can be measured in triplicates each time.

For the hemocompatibility studies, statistical analysis was performed where possible. However, at a maximum, blood from 3 different donors was used. For stronger results, it is recommended to conduct hemocompatibility results on blood from more donors. For cell viability, the assays should be repeated to the point of at least 3 biological and 3 technical replicates per biological replicate.

8.2 Position of the research in the field of OGBs

OGBs are an interesting line of research for many applications, as mentioned in section 3.2.4. Many studies have attempted to create oxygen-generating materials, largely based on CPO. It is interesting to compare the achievements from similar constructs, as the oxygen-generation is based on the same principle.

Constructs based on PCL and CPO have been fabricated in numerous studies [15, 59, 66]. Oxygen release was reported for up to 14 days. What distinguishes some of these works from this research is that the MPs are embedded in hydrogels, such as GelMa. Suvarnapathaki et al. accepted larger sizes for the MPs, stating an average of 100 μm. This may be an important factor for encapsulating sufficient CPOs to acquire such a prolonged release [59]. Morais et al. have produced OG-PCLs with average sizes of 46 μm, which decreased to 17 μm when adding a stabilizer [46]. However,

other studies have managed to produce OG-PCL MPs between 1-10 μm. It is worth investigating if the protocol in this study can be adapted using elements from these studies. Techniques such as single emulsions or electrospraying have been used in these similar works. Issues with CPO encapsulation were not mentioned.

Other hydrophobic polymers can also be employed for the encapsulation of CPO, as hydrophobic materials slow down the hydrolytic degradation. Examples of these materials are polylactic acid (PLA), poly (L-lactic acid), and poly (lactide-co-glyclide). Numerous studies have been conducted on the combination of CPO with these materials, and prolonged oxygen release was measured for all mentioned constructs. Hence, it is interesting to explore these materials. The addition of catalase and lipid coatings can also be translated to these substrates.

An interesting candidate for oxygen therapeutics is PLA. Khorshidi et al. have developed oxygen-generating CPO-based PLA MPs, which were added to hydrogels to create composites for chondrogenic differentiation [28]. These PLA-CPO MPs could be interesting to investigate in more detail, as PLA is more deformable than PCL, and can also be coated. The combination of PLA and CPO was also explored by Mohammed et al., who developed 3D-printed PLA-CPO filaments [42].

Poly (L-lactic acid) has been combined with CPOs and catalase to fabricate OG MPs, which were reported to release oxygen for up to 15 days [43]. They explored solid-filled and hollow MPs, fabricated with nano CPOs. Catalase was grafted on the surface and prevented cytotoxicity. Grafting is an interesting incorporation method for the constructs in this work. Carboxylic groups were introduced on the surface of the MPs and catalase was added to introduced hydroxysuccinimide esters via its lysine residues. The hydroxysuccinimide esters were coupled to the catalase lysine residues by incubation together for 4 hours. This linking is similar to the catalase-conjugation to Alexa Fluor™ 488 in this work. MP sizes ranged from 57 to 125 μm, depending on the ratios of poly (L-lactic acid) and CPO.

Poly (lactide-co-glyclide) has been combined with nano CPOs into biconcave MPs in another work by Khorshidi et al. Surface modifications were possible, so this could be an interesting construct for coating with the CT lipid formulation. The biconcave shape and diameter of 5.3 μm make this work an interesting candidate for RBC substitution. The particles were able to generate oxygen for 14 days, however, the amounts were accepted for bone tissue engineering, which is an hypoxic evironment [29]. Another work using poly (lactide-co-glyclide) explored catalase-containing OG-MPs, with the goal of downregulating hypoxia-inducible factors in rat cardiomyocytes. Oxygen release was detected for 24 hours and hypoxia-induced myocardial injuries were reduced [37].

Compared to other publications in the field, the developed CO-OG-PCL MPs release minor and short-term oxygen. By adapting the protocols, this release can be increased and prolonged. However, this work has novelty and strength in the addition of erythrocyte-inspired synthetic lipid coatings, in addition to the catalase coating. While the combination of complex lipid formulations and catalase does not work, an alternative formulation is proposed, which is a promising candidate for further development. The research regarding bio-inspired lipid formulations and alternatives to PEG is what provided new, useful insights in the field of RBC substitution, and gives a direction for the continuation of this work. This is not only useful for RBC substitutes, but can also be translated to the wide field of intravenous drug development and delivery. As erythrocytes are naturally occurring in the bloodstream, no immune response is generated against them. Using this membrane as an inspiration and closely mimicking it with synthetic lipids is a promising way of improving the hemocompatibility of any micro or nanocarrier. The lipid coatings can be adapted for numerous other materials or drug-encapsulated materials. At this point, synthetic lipid-based erythrocyte-inspired coatings are not widely researched. This work is novel in this regard and

although this work focuses on the application of these membranes in oxygen therapeutics, the possibilities go way beyond that.

8.3 Recommendations for further development of the constructs

The MPs in this research were designed with the goal of serving as erythrocyte substitutes. There is extensive research to be conducted and adjustments to the MP design to be made, in order to develop a therapy that is both functional and safe for this intended purpose. At its current stage, the application of these MPs for erythrocyte substitution is not feasible. The particles have not successfully encapsulated sufficient amounts of CPO and catalase at their current size range, and complex lipid formulations were not stable. This research has provided valuable insights and information regarding aspects that work and do not work, and has highlighted areas for improvement.

It is worthwhile to explore other materials for encapsulating CPOs and catalase. As PCL is stiff and non-deformable, very small particles need to be fabricated to ensure the safety of intravenous delivery. At 5 μm, the risk of capillary obstruction or retention within vasculature remains a concern. Perfusion tests on vessels-on-a-chip or in microcapillaries can be employed to assess the risk and extent to which this could happen. Furthermore, encapsulating sufficient amounts of CPO within these MPs has been proven difficult. The encapsulation process of CPOs has to be optimized first, before continuing with other aspects of the constructs. Since the CPOs tend to aggregate, they are likely too large for encapsulation in the PCL. Nano CPOs can be fabricated and possibly encapsulated in larger PCLs. Larger oxygen-generating PCL MPs are interesting oxygen-therapeutics for *ex-vivo* purposes, like tissue engineering. They can be used to oxygenate engineered tissue constructs and organoids, or administer oxygen in organ transplants to enhance their survival *ex-vivo*. For this purpose, the MPs would be used to prevent ischemia. It is also interesting to study the potential of the particles to reverse damage in hypoxic and ischemic tissue models.

As aforementioned, other hydrophobic polymers have achieved promising results in the field. It would be valuable to explore these materials. Other materials, such as hydrogels, should also be considered. Hydrogels can be fabricated with similar deformability to erythrocytes. Additionally, softer materials will be able to squeeze through capillaries. Microgels are excellent candidates for this. Microgels can be fabricated with similar size ranges as erythrocytes and can be modified in composition to acquire specific characterizations, such as deformability, porosity, and stiffness. CPO and catalase can be incorporated into the polymer networks.

As the strength of this research lies in the addition of catalase and a lipid coating, this work should be translated to these other substrates. From this current research, it is known that the CT formulation forms well-formed coatings on catalase-coated MPs. It is highly encouraged to continue to improve the hemocompatibility of the constructs through these coatings, perhaps in comparison with a PEGylated analog.

9 Conclusion

In this work, lipid-coated, catalase-containing oxygen-generating PCL MPs were produced, as a potential erythrocyte substitutes in blood transfusions. The MPs were produced with small size ranges, below biological erythrocytes. This work has shown that encapsulation of sufficient amounts of CPOs is difficult at this stage of research. OG-PCL MPs released H_2O_2 for up to 50 hours and minor amounts for O_2 for up to 46 hours. However, the oxygen release detection methods seemed partly disturbed by PCL and therefore, the release has to be assessed again using other, more reliable mechanisms. When continuing with PCL as a substrate for encapsulation of CPOs, it is recommended to investigate other protocols for producing the MPs and to increase the size range of the MPs. It is also worthwhile to explore other hydrophobic polymers or microgels.

The OG-PCL MPs were coated with catalase as an antioxidant. After incorporation or coating with catalase, the calatytic activity was proven by a decrease in H_2O_2 release. Catalase coated MPs did no longer show an initial burst of H_2O_2, thus lowering the cytotoxicity of the MPs. The addition of catalase to OG-PCL MPs is key to producing hemocompatible MPs. To further improve the hemocompatibility, erythrocyte-mimicking lipid coatings were added to the constructs. This study has provided useful insights into the combination of erythrocyte-inspired lipid coatings and catalase. Multiple formulations were tested with varying rates of complexity. It has been assessed that although SM-containing lipid formulations do not properly form coatings on CO-OG-PCLs, the addition of these coatings does lower the induced blood immune response to MPs. A less complex CT formulation was able to form stealthy, well-defined coatings and is recommended for usage in further studies with regard to increasing the hemocompatibility of MPs.

To conclude, lipid-coated, catalase-containing oxygen-generating PCL MPs can be produced using the double emulsion method described in this thesis, however, as the oxygen-generating capacity is low, it is recommended to alter the protocol or materials according to the recommendations and insights provided by this thesis. The novelty of combining a catalase layer with erythrocyte-inspired coatings is encouraged to be continued in further studies.

References

[1] Abdi, S. I. H., Ng, S. M., and Lim, J. O. (2011). An enzyme-modulated oxygen-producing microsystem for regenerative therapeutics. *International Journal of Pharmaceutics*, 409(1-2):203–205.

[2] Aharoni, R. and Tobi, D. (2018). Dynamical comparison between myoglobin and hemoglobin. *Proteins: Structure, Function, and Bioinformatics*, 86(11):1176–1183.

[3] Allevi 3D systems (2022). Live/Dead Quantification Using Fiji - Step-by-Step Guide.

[4] Asghar, H. (2022). Blood Substitutes Current Options , Scope and Future Prospects : A Brief Review. 14(8):1–8.

[5] Basu, D. and Kulkarni, R. (2014). Overview of blood components and their preparation. *Indian Journal of Anaesthesia*, 58(5):529.

[6] Brieger, K., Schiavone, S., Miller, F. J., and Krause, K. H. (2012). Reactive oxygen species: From health to disease. *Swiss Medical Weekly*, 142(August):1–14.

[7] Buchwald, H., O'Dea, T. J., Menchaca, H. J., Michalek, V. N., and Rohde, T. D. (2000). Effect Of Plasma Cholesterol On Red Blood Cell Oxygen Transport. *Clinical and Experimental Pharmacology and Physiology*, 27(12):951–955.

[8] Chang, C.-J., Chen, C.-H., Chen, B.-M., Su, Y.-C., Chen, Y.-T., Hershfield, M. S., Lee, M.-T. M., Cheng, T.-L., Chen, Y.-T., Roffler, S. R., and Wu, J.-Y. (2017). A genome-wide association study identifies a novel susceptibility locus for the immunogenicity of polyethylene glycol. *Nature Communications*, 8(522).

[9] Charbe, N. B., Castillo, F., Tambuwala, M. M., Prasher, P., Chellappan, D. K., Carreño, A., Satija, S., Singh, S. K., Gulati, M., Dua, K., González-Aramundiz, J. V., and Zacconi, F. C. (2022). A new era in oxygen therapeutics? From perfluorocarbon systems to haemoglobin-based oxygen carriers. *Blood Reviews*, 54(January).

[10] Cohn, C. S. and Cushing, M. M. (2009). Oxygen Therapeutics: Perfluorocarbons and Blood Substitute Safety. *Critical Care Clinics*, 25(2):399–414.

[11] Diez-Silva, M., Dao, M., Han, J., Lim, C. T., and Suresh, S. (2010). Shape and biomechanics characteristics of human red blood cells in health and disease. *MRS Bulletin*, 35(5):382–388.

[12] Ding, R., Hase, Y., Ameen-Ali, K. E., Ndung'u, M., Stevenson, W., Barsby, J., Gourlay, R., Akinyemi, T., Akinyemi, R., Uemura, M. T., Polvikoski, T., Mukaetova-Ladinska, E., Ihara, M., and Kalaria, R. N. (2020). Loss of capillary pericytes and the blood–brain barrier in white matter in poststroke and vascular dementias and Alzheimer's disease. *Brain Pathology*, 30(6):1087–1101.

[13] Elahi, M. F., Guan, G., Wang, L., and King, M. W. (2014). Improved hemocompatibility of silk fibroin fabric using layer-by-layer polyelectrolyte deposition and heparin immobilization. *Journal of Applied Polymer Science*, 131(18):9307–9318.

[14] Erikson, K. M. and Aschner, M. (2019). Manganese: Its Role in Disease and Health. *Metal Ions in Life Sciences*, 19:253–266.

[15] Farzin, A., Hassan, S., Moreira Teixeira, L. S., Gurian, M., Crispim, J. F., Manhas, V., Carlier, A., Bae, H., Geris, L., Noshadi, I., Shin, S. R., and Leijten, J. (2021). Self-Oxygenation of Tissues Orchestrates Full-Thickness Vascularization of Living Implants. *Advanced Functional Materials*, 31(42).

[16] Ferhan, A. R., Yoon, B. K., Park, S., Sut, T. N., Chin, H., Park, J. H., Jackman, J. A., and Cho, N. J. (2019). Solvent-assisted preparation of supported lipid bilayers. *Nature Protocols*, 14(7):2091–2118.

[17] García-álvarez, R. and Vallet-Regí, M. (2021). Hard and soft protein corona of nanomaterials: Analysis and relevance. *Nanomaterials*, 11(4).

[18] Gholipourmalekabadi, M., Zhao, S., Harrison, B. S., Mozafari, M., and Seifalian, A. M. (2016). Oxygen-Generating Biomaterials: A New, Viable Paradigm for Tissue Engineering? *Trends in Biotechnology*, 34(12):1010–1021.

[19] Giarratana, M. C., Rouard, H., Dumont, A., Kiger, L., Safeukui, I., Le Pennec, P. Y., François, S., Trugnan, G., Peyrard, T., Marie, T., Jolly, S., Hebert, N., Mazurier, C., Mario, N., Harmand, L., Lapillonne, H., Devaux, J. Y., and Douay, L. (2011). Proof of principle for transfusion of in vitro-generated red blood cells. *Blood*, 118(19):5071–5079.

[20] Haddad, H. F., Burke, J. A., Scott, E. A., and Ameer, G. A. (2022). Clinical Relevance of Pre-Existing and Treatment-Induced Anti-Poly (Ethylene Glycol) Antibodies. *Regenerative Engineering and Translational Medicine*, 8:32–42.

[21] Harrison, B. S., Eberli, D., Lee, S. J., Atala, A., and Yoo, J. J. (2007). Oxygen producing biomaterials for tissue regeneration. *Biomaterials*, 28(31):4628–4634.

[22] Hohner, A. O., David, M. P. C., and Rädler, J. O. (2010). Controlled solvent-exchange deposition of phospholipid membranes onto solid surfaces. *Biointerphases*, 5(1):1–8.

[23] Hsieh, T. E., Lin, S. J., Chen, L. C., Chen, C. C., Lai, P. L., and Huang, C. C. (2020). Optimizing an Injectable Composite Oxygen-Generating System for Relieving Tissue Hypoxia. *Frontiers in Bioengineering and Biotechnology*, 8(May):1–10.

[24] Hu, K., Martorell mmartorell, M., udeccl Daniela Calina, Cho, W. C., Sharifi-Rad, J., Kumar, A. N., Fokou, T. P., Mishra, P. A., Rayess, E. Y., Sharifi-Rad, M., Anil Kumar, N. V., Zucca, P., Maria Varoni, E., Dini, L., Panzarini, E., Rajkovic, J., Valere Tsouh Fokou, P., Azzini, E., Peluso, I., Prakash Mishra, A., Nigam, M., El Rayess, Y., El Beyrouthy, M., Polito, L., Iriti, M., Martins, N., Martorell, M., Oana Docea, A., Setzer, W. N., and Calina, D. (2020). Lifestyle, Oxidative Stress, and Antioxidants: Back and Forth in the Pathophysiology of Chronic Diseases. *Front. Physiol*, 11:694.

[25] ISO (2009). ISO 10993-5:2009 - Biological evaluation of medical devices — Part 5: Tests for in vitro cytotoxicity.

[26] Jansman, M. M. T., Coll-Satue, C., Liu, X., Kempen, P. J., Andresen, T. L., Thulstrup, P. W., and Hosta-Rigau, L. (2022). Hemoglobin-based oxygen carriers camouflaged with membranes extracted from red blood cells: Optimization and assessment of functionality. *Biomaterials Advances*, 134(January):112691.

[27] Kaye, A. D., Samaniego, K., Miriyala, S., Miller, B. C., Cornett, E. M., and Conrad, S. A. (2022). Perfluorocarbon-Based Oxygen Carriers. pages 175–179.

[28] Khorshidi, S., Karimi-Soflou, R., and Karkhaneh, A. (2021). A hydrogel/particle composite with a gradient of oxygen releasing microparticle for concurrent osteogenic and chondrogenic differentiation in a single scaffold. *Colloids and Surfaces B: Biointerfaces*, 207(April):112007.

[29] Khorshidi, S., Karkhaneh, A., and Bonakdar, S. (2020). Fabrication of amine-decorated nonspherical microparticles with calcium peroxide cargo for controlled release of oxygen. *Journal of biomedical materials research. Part A*, 108(1):136–147.

[30] Kozma, G. T., Shimizu, T., Ishida, T., and Szebeni, J. (2020). Anti-PEG antibodies: Properties, formation, testing and role in adverse immune reactions to PEGylated nano-biopharmaceuticals.

[31] Kumašin, A., Mahmutović, L., and Hromić-Jahjefendić, A. (2022). Testing temperature and pH stability of the catalase enzyme in the presence of inhibitors. *Periodicals of Engineering and Natural Sciences*, 10(2):18–29.

[32] La-Beck, N. M., Islam, M. R., and Markiewski, M. M. (2021). Nanoparticle-Induced Complement Activation: Implications for Cancer Nanomedicine. *Frontiers in Immunology*, 11(January):1–12.

[33] Liu, H., Kaye, A. D., and Jahr, J. S. (2022). *Blood Substitutes and Oxygen Biotherapeutics*. Springer Cham, 1 edition.

[34] Liu, N., Wu, A. H., and Wong, S. S. (1993). Improved quantitative Apt test for detecting fetal hemoglobin in bloody stools of newborns. *Clinical Chemistry*, 39(11):2326–2329.

[35] Lorent, J. H., Levental, K. R., Ganesan, L., Rivera-Longsworth, G., Sezgin, E., Doktorova, M., Lyman, E., and Levental, I. (2020). Plasma membranes are asymmetric in lipid unsaturation, packing and protein shape. *Nature Chemical Biology*, 16(6):644–652.

[36] Malachowski, T. and Hassel, A. (2020). Engineering nanoparticles to overcome immunological barriers for enhanced drug delivery. *Engineered Regeneration*, 1(June):35–50.

[37] Mandal, K., Sangabathuni, S., Haghniaz, R., Kawakita, S., Mecwan, M., Nakayama, A., Zhang, X., Edalati, M., Huang, W., Lopez Hernandez, A., Jucaud, V., Dokmeci, M. R., and Khademhosseini, A. (2023). Oxygen-generating microparticles downregulate HIF-1α expression, increase cardiac contractility, and mitigate ischemic injury. *Acta biomaterialia*, 159:211–225.

[38] Marmur, A., Volpe, C. D., Siboni, S., Amirfazli, A., and Drelich, J. W. (2017). Contact angles and wettability: Towards common and accurate terminology. *Surface Innovations*, 5(1):3–8.

[39] McGann, P. T. and Weyand, A. C. (2022). Lessons learned from the COVID-19 pandemic blood supply crisis. *Journal of Hospital Medicine*, 17(7):574–576.

[40] Mellman, W. J., Schimke, R. T., and Hayflick, L. (1972). Catalase turnover in human diploid cell cultures. *Experimental Cell Research*, 73(2):399–409.

[41] Mohamed, M., Elsadek, N., Emam, S., hamdy Abdelkader, Farghaly, U., and Sarhan, H. (2022). Complement activation-related pseudo allergy of PEGylated products: Safety aspects, models, the role of anti-PEG antibodies, and ways to overcome. *Journal of advanced Biomedical and Pharmaceutical Sciences*, 5(2):79–87.

[42] Mohammed, A., Saeed, A., Elshaer, A., Melaibari, A. A., Memić, A., Hassanin, H., and Essa, K. (2023). Fabrication and Characterization of Oxygen-Generating Polylactic Acid/Calcium Peroxide Composite Filaments for Bone Scaffolds. *Pharmaceuticals*, 16(4).

[43] Mohseni-Vadeghani, E., Karimi-Soflou, R., Khorshidi, S., and Karkhaneh, A. (2021). Fabrication of oxygen and calcium releasing microcarriers with different internal structures for bone tissue engineering: Solid filled versus hollow microparticles. *Colloids and Surfaces B: Biointerfaces*, 197.

[44] Montazeri, L., Hojjati-Emami, S., Bonakdar, S., Tahamtani, Y., Hajizadeh-Saffar, E., Noori-Keshtkar, M., Najar-Asl, M., Ashtiani, M. K., and Baharvand, H. (2016). Improvement of islet engrafts by enhanced angiogenesis and microparticle-mediated oxygenation. *Biomaterials*, 89:157–165.

[45] Moradi, S., Jahanian-Najafabadi, A., and Roudkenar, M. H. (2016). Artificial blood substitutes: First steps on the long route to clinical utility. *Clinical Medicine Insights: Blood Disorders*, 9:33–41.

[46] Morais, A. I., Wang, X., Vieira, E. G., Viana, B. C., Silva-Filho, E. C., Osajima, J. A., Afewerki, S., Corat, M. A., Silva, H. S., Marciano, F. R., Ruiz-Esparza, G. U., Stocco, T. D., de Paula, M. M., and Lobo, A. O. (2020). Electrospraying oxygen-generating microparticles for tissue engineering applications. *International Journal of Nanomedicine*, 15:1173–1186.

[47] Niesor, E. J., Nader, E., Perez, A., Lamour, F., Benghozi, R., Remaley, A., Thein, S. L., and Connes, P. (2022). Red Blood Cell Membrane Cholesterol May Be a Key Regulator of Sickle Cell Disease Microvascular Complications. *Membranes*, 12(11).

[48] Papini, E., Tavano, R., and Mancin, F. (2020). Opsonins and Dysopsonins of Nanoparticles: Facts, Concepts, and Methodological Guidelines. *Frontiers in Immunology*, 11(October):1–19.

[49] Qi, C., Chen, Y., Jing, Q. Z., and Wang, X. G. (2011). Preparation and characterization of catalase-loaded solid lipid nanoparticles protecting enzyme against proteolysis. *International Journal of Molecular Sciences*, 12(7):4282–4293.

[50] Rafique, M., Ali, O., Shafiq, M., Yao, M., Wang, K., Ijima, H., Kong, D., and Ikeda, M. (2023). Insight on Oxygen-Supplying Biomaterials Used to Enhance Cell Survival, Retention, and Engraftment for Tissue Repair. *Biomedicines*, 11(6):1–24.

[51] Rastinfard, A., Dalisson, B., and Barralet, J. (2022). Aqueous decomposition behavior of solid peroxides: Effect of pH and buffer composition on oxygen and hydrogen peroxide formation. *Acta Biomaterialia*, 145:390–402.

[52] Ray, P. D., Huang, B. W., and Tsuji, Y. (2012). Reactive oxygen species (ROS) homeostasis and redox regulation in cellular signaling. *Cellular Signalling*, 24(5):981–990.

[53] Richter, A. W. and Åkerblom, E. (1984). Polyethylene Glycol Reactive Antibodies in Man: Titer Distribution in Allergic Patients Treated with Monomethoxy Polyethylene Glycol Modified Allergens or Placebo, and in Healthy Blood Donors. *International Archives of Allergy and Applied Immunology*, 74(1):36–39.

[54] Roghani, K., Holtby, R., and Jahr, J. (2014). Effects of Hemoglobin-Based Oxygen Carriers on Blood Coagulation. *Journal of Functional Biomaterials*, 5(4):288–295.

[55] Schubert, A., O'Hara, J. F., Przybelski, R. J., Tetzlaff, J. E., Marks, K. E., Mascha, E., and Novick, A. C. (2002). Effect of diaspirin crosslinked hemoglobin (DCLhb HemAssist™) during high blood loss surgery on selected indices of organ function. *Artificial Cells, Blood Substitutes, and Immobilization Biotechnology*, 30(4):259–283.

[56] Strayer, D. S. and Rubin, E. (2015). *Rubin's pathology: Clinicopathologic Foundations of Medicine*. Wolters Kluwer, 7 edition.

[57] Sushnitha, M., Evangelopoulos, M., Tasciotti, E., and Taraballi, F. (2020). Cell Membrane-Based Biomimetic Nanoparticles and the Immune System: Immunomodulatory Interactions to Therapeutic Applications. *Frontiers in Bioengineering and Biotechnology*, 8(June):1–17.

[58] Suvarnapathaki, S., Wu, X., Lantigua, D., Nguyen, M. A., and Camci-Unal, G. (2019). Breathing life into engineered tissues using oxygen-releasing biomaterials. *NPG Asia Materials*, 11(1).

[59] Suvarnapathaki, S., Wu, X., Zhang, T., Nguyen, M. A., Goulopoulos, A. A., Wu, B., and Camci-Unal, G. (2022). Oxygen generating scaffolds regenerate critical size bone defects. *Bioactive Materials*, 13(September 2021):64–81.

[60] Tantawi, O., Baalbaki, A., El Asmar, R., and Ghauch, A. (2019). A rapid and economical method for the quantification of hydrogen peroxide (H2O2) using a modified HPLC apparatus. *Science of The Total Environment*, 654:107–117.

[61] Thanh, T., Thi, H., Pilkington, E. H., Nguyen, D. H., and Lee, J. S. (2020). The Importance of Poly (ethylene glycol) Alternatives for Overcoming PEG Immunogenicity in Drug. *Polymers*, 12(2):298.

[62] Touri, M., Moztarzadeh, F., Osman, N. A. A., Dehghan, M. M., and Mozafari, M. (2018). 3D–printed biphasic calcium phosphate scaffolds coated with an oxygen generating system for enhancing engineered tissue survival. *Materials Science and Engineering C*, 84(May 2017):236–242.

[63] Trakarnsanga, K., Griffiths, R. E., Wilson, M. C., Blair, A., Satchwell, T. J., Meinders, M., Cogan, N., Kupzig, S., Kurita, R., Nakamura, Y., Toye, A. M., Anstee, D. J., and Frayne, J. (2017). An immortalized adult human erythroid line facilitates sustainable and scalable generation of functional red cells. *Nature Communications*, 8(May 2016).

[64] Wang, Z., Hood, E. D., Nong, J., Ding, J., Marcos-Contreras, O. A., Glassman, P. M., Rubey, K. M., Zaleski, M., Espy, C. L., Gullipali, D., Miwa, T., Muzykantov, V. R., Song, W. C., Myerson, J. W., and Brenner, J. S. (2022). Combating Complement's Deleterious Effects on Nanomedicine by Conjugating Complement Regulatory Proteins to Nanoparticles. *Advanced Materials*, 34(8):1–12.

[65] Wenzel, R. N. (1936). Resistance of solid surfaces to wetting by water. *Industrial and Engineering Chemistry*, 28(8):988–994.

[66] Willemen, N. G., Hassan, S., Gurian, M., Jasso-Salazar, M. F., Fan, K., Wang, H., Becker, M., Allijn, I. E., Bal-Öztürk, A., Leijten, J., and Shin, S. R. (2022). Enzyme-Mediated Alleviation of Peroxide Toxicity in Self-Oxygenating Biomaterials. *Advanced Healthcare Materials*, 11(13):1–13.

[67] Willemen, N. G., Hassan, S., Gurian, M., Li, J., Allijn, I. E., Shin, S. R., and Leijten, J. (2021). Oxygen-Releasing Biomaterials: Current Challenges and Future Applications. *Trends in Biotechnology*, 39(11):1144–1159.

[68] World Health Organization (2021). *Global status report on blood safety and availability*.

[69] Yang, Q., Jacobs, T. M., McCallen, J. D., Moore, D. T., Huckaby, J. T., Edelstein, J. N., and Lai, S. K. (2016). Analysis of pre-existing IgG and IgM antibodies against polyethylene glycol (PEG) in the general population. *Analytical Chemistry*, 88(23):11804–11812.

[70] Yang, Q. and Lai, S. K. (2015). Anti-PEG immunity: Emergence, characteristics, and unaddressed questions. *Wiley Interdisciplinary Reviews: Nanomedicine and Nanobiotechnology*, 7(5):655–677.

[71] Younus, H. (2018). Younus, H. (2018). Therapeutic potentials of superoxide dismutase. . *International journal of health sciences*, 12(3):88–93.

[72] Zhu, W., Dong, Z., Fu, T., Liu, J., Chen, Q., Li, Y., Zhu, R., Xu, L., and Liu, Z. (2016). Modulation of Hypoxia in Solid Tumor Microenvironment with MnO2 Nanoparticles to Enhance Photodynamic Therapy. *Advanced Functional Materials*, 26(30):5490–5498.

[73] Zwaal, R. F., Comfurius, P., and Bevers, E. M. (1998). Lipid-protein interactions in blood coagulation. *Biochimica et Biophysica Acta - Reviews on Biomembranes*, 1376(3):433–453.

10 Appendices

A Additional results H_2O_2 measurements

A.1 Additional data H_2O_2 release of OG-PCL and CO-OG-PCL

An additional batch of OG-PCL and CO-OG-PCL was analyzed. The release kinetics are similar to the results presented in the thesis. Due to the low reproducibility of the H_2O_2 studies, the acquired data from multiple batches can't be combined and used for statistical analyses.

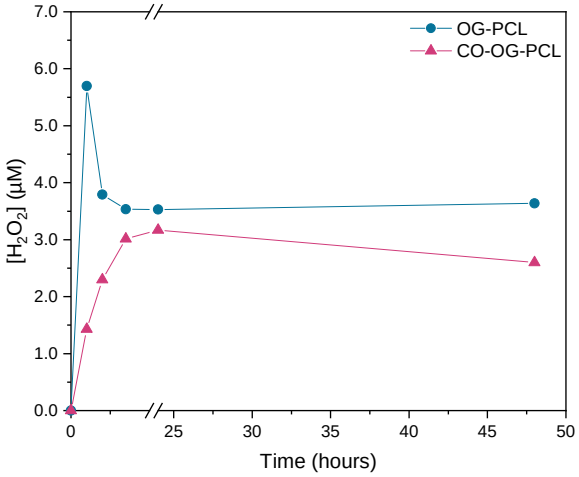

Figure 17 *H_2O_2 release of another batch of OG-PCL and CO-OG-PCL.*

A.2 Supporting data H_2O_2 release of lipid-coated MPs

In this Appendix, additional results from H_2O_2 release studies on lipid-coated OG-PCL and CO-OG-PCL MPs are shown. These data support the claims made in section 8.1.1) Multiple factors introduced error margins into these results. This Appendix highlights the poor reproducibility of the H_2O_2 assay. Issues that were found include:

- Low reproducibility when creating standard curve (enzymatic sensitivity and variations)
- Poor linear fit, sometimes a second-degree polynomial was necessary
- Poor fitting to the curve in the lower concentrations (0-5 µM), resulting in negative values
- Very low H_2O_2 concentrations in the samples, resulting in a low stability of H_2O_2
- Autofluorescence of PCL in the resorufin spectrum
- Varying MP concentrations between samples
- Varying CPO and catalase concentrations between samples

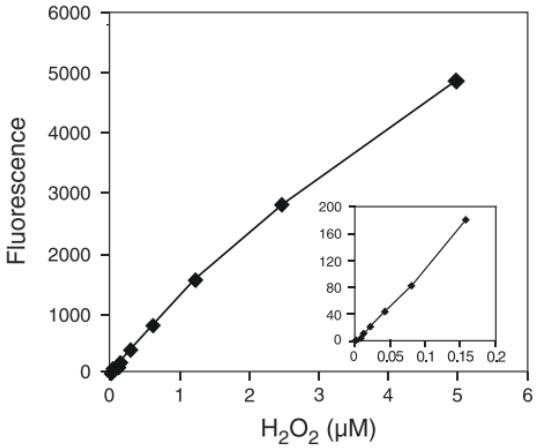

Figure 18 *The standard curve of the H_2O_2 Amplex Red kit, as shown in the user guide provided by Invitrogen. Invitrogen states that this curve can be described with a linear fit.*

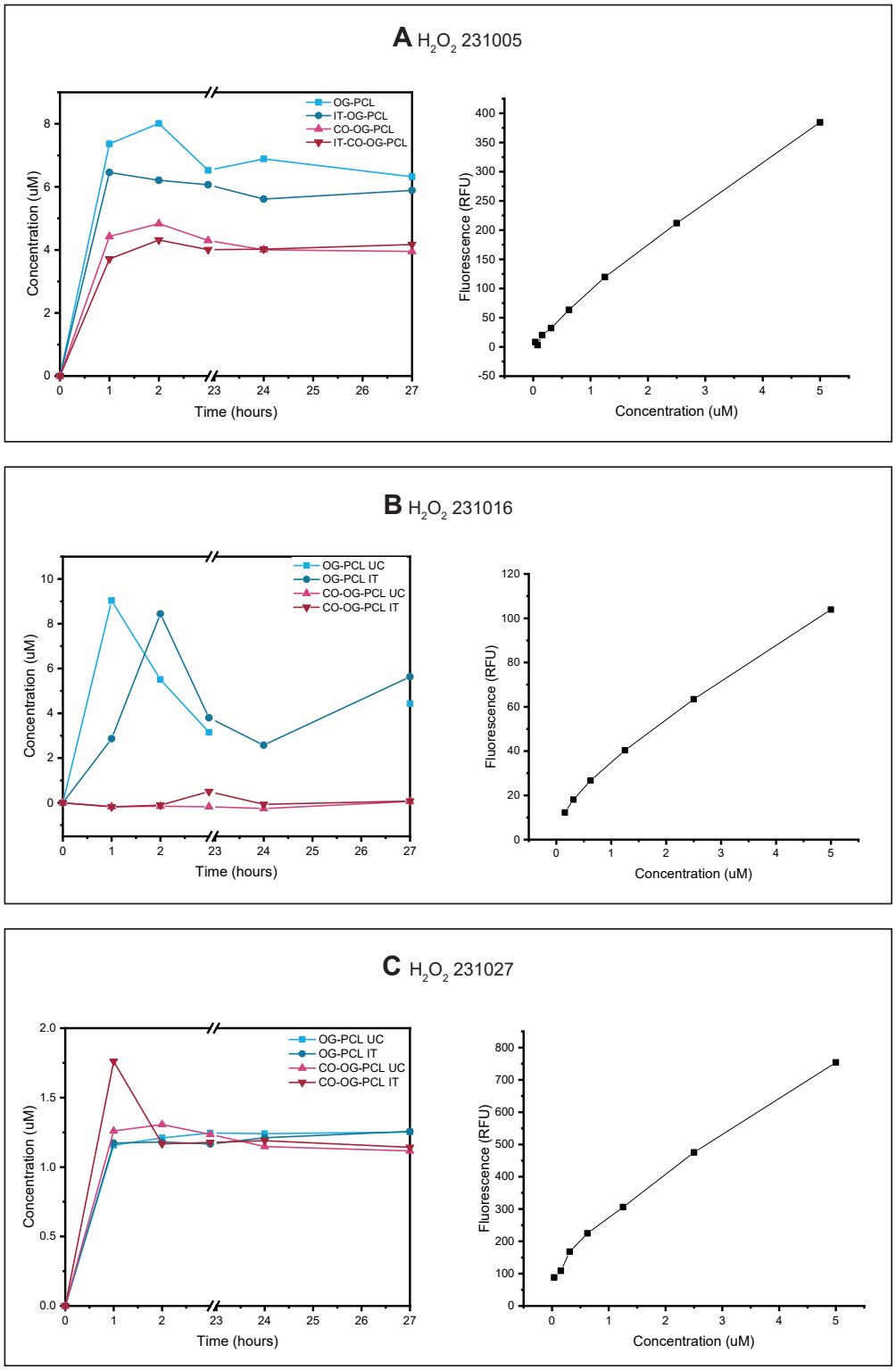

Figure 19 *Multiple H_2O_2 studies on lipid-coated particles and the results. **A** H_2O_2 study conducted on 05/10/23. The standard curve could be described with a linear fit. The data points fit within the linear range. The final results have taken into account the dilution factor of 20. **B** H_2O_2 study conducted on 16/10/23. The CO-OG-PCL samples had a too low particle concentration, despite efforts to even out all concentrations. As a result, little H_2O_2 was present in the samples, which may have been overshadowed by the autofluorescence of PCL. After fitting to the curve, the values ended up lower than the blanks. **C** H_2O_2 study conducted on 27/10/23. All MP concentrations were low. After correcting for the dilution factor, detected H_2O_2 concentrations were still below 2 uM. Data points did not fit properly to the standard curve, and the standard curve is unreliable in the lower concentrations.*

B Supporting data optical oxygen measurements

This graph supports the discussion of the optical oxygen measurements (section 8.1.2). The measurement was started under stirring, 50 RPM. At some point, the stirring was turned off. The signal increased again, demonstrating that PCL interacts with the optical oxygen measurement.

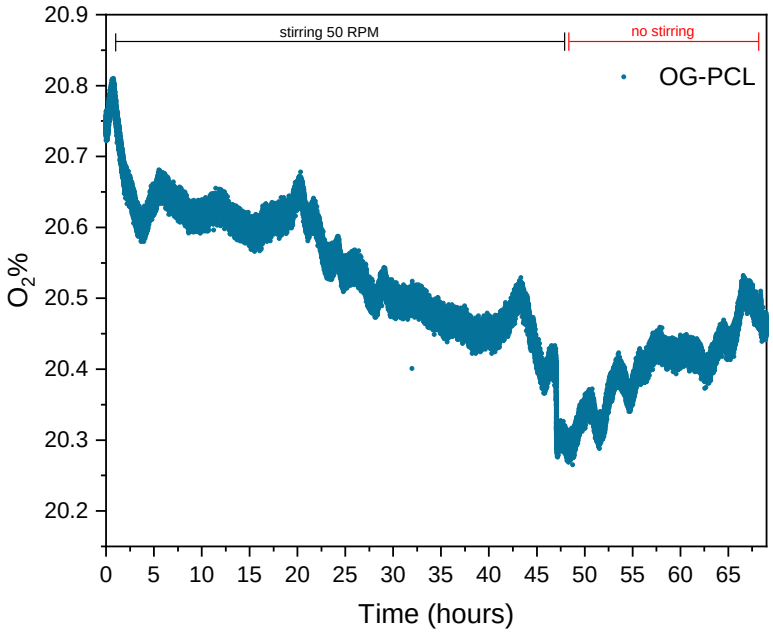

Figure 20 *Optical oxygen release of OG-PCL MPs, measured whilst stirring under physiological O_2%.*

C Supporting data electrochemical oxygen measurements

These graphs support the discussion of the electrochemical oxygen measurements (section 8.1.2). Fig. 21B shows that at roughly 1.5 hours, the stirring of OG-PCL was changed from 2 to 3 mot. The signal increases, suggesting that PCL particles interact with the probe.

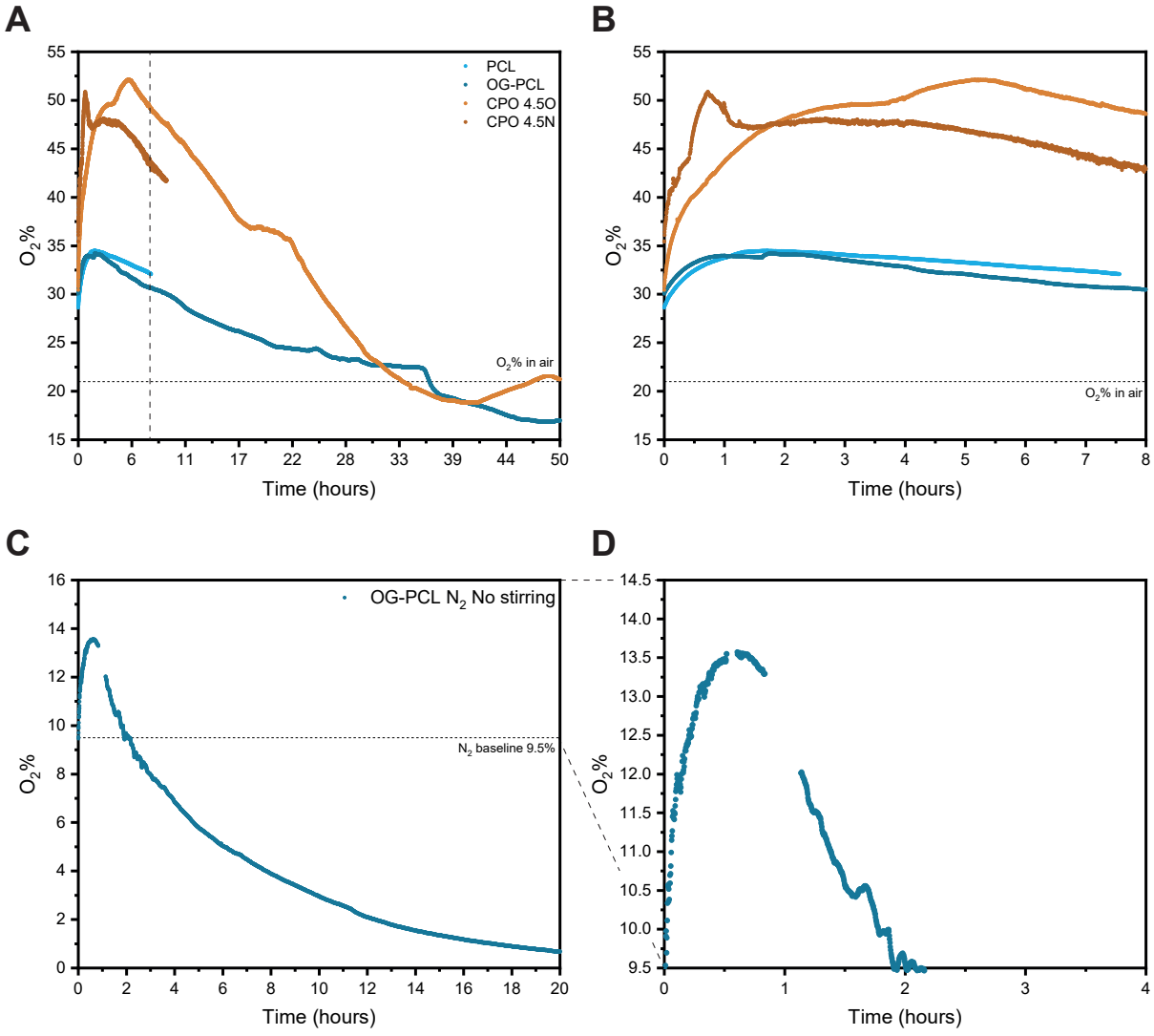

Figure 21 *Additional electrochemical oxygen measurements, measured while stirring, under physiological O_2%. **A** Oxygen release of CPO 4.5 mg (a new batch of powder (CPO 4.5N) and an older batch of powder (CPO 4.5O), OG-PCL and PCL **B** A close-up of the first 8 hours of A. **C** Oxygen measurements of OG-PCL under nitrogen atmosphere **D** A close-up of the release of C. between the baseline and the peak. Data points are missing as the laptop went to sleep.*

D Supplementary microscopy images of the coatings

D.1 Fluorescence microscopy of coated PCL MPs

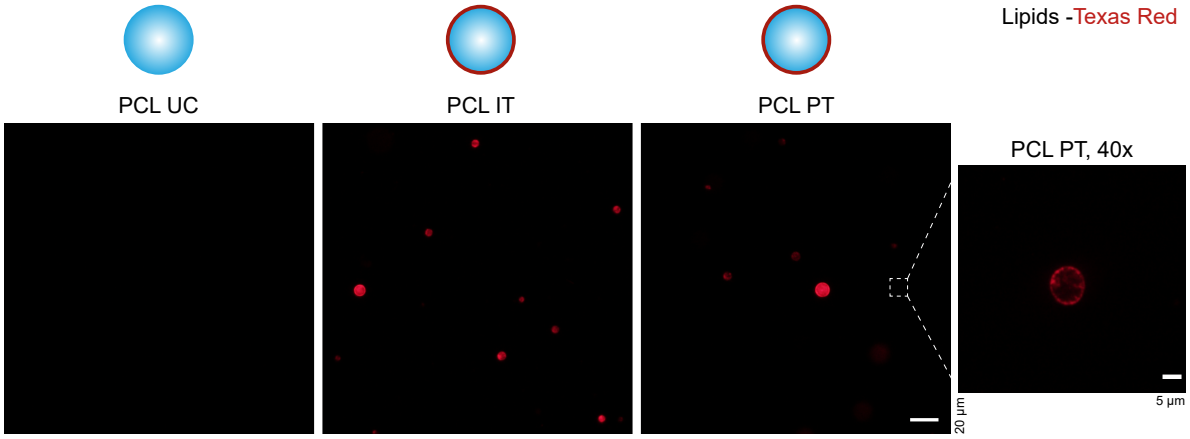

Figure 22 *Fluorescence microscopy of coated and uncoated PCL MPs.*

D.2 Confocal microscopy of CT-coated CO-OG-PCL MPs, coated using adapted SALB without heating

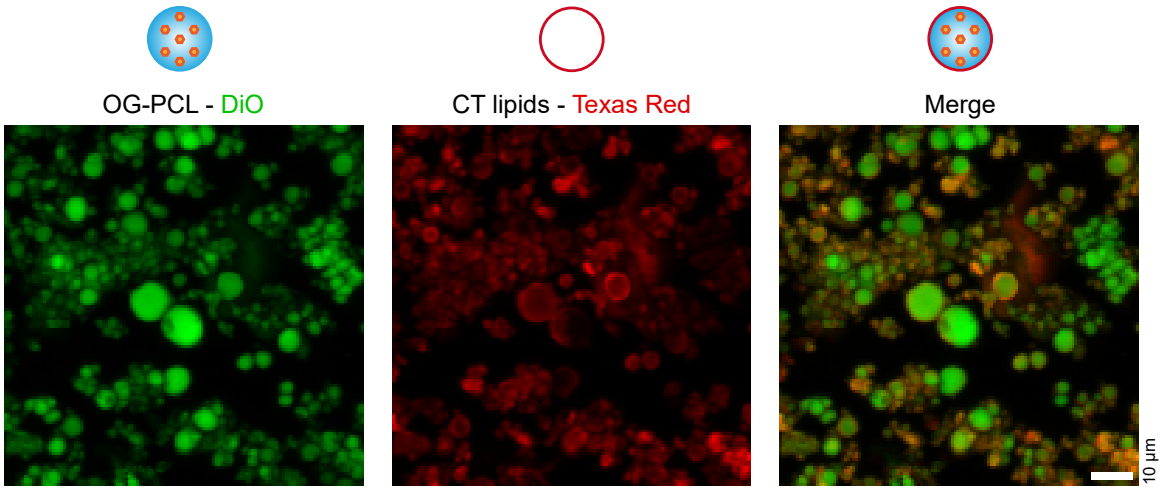

Figure 23 *Confocal microscopy of CT-CO-OG-PCLs, coated using the adapted SALB protocol without heating.*
The different channels were imaged separately and merged. The coatings are well-established around the particles and the coating efficiency is high: almost all particles are coated.

E Additional data C5a and IgG activation assays per donor

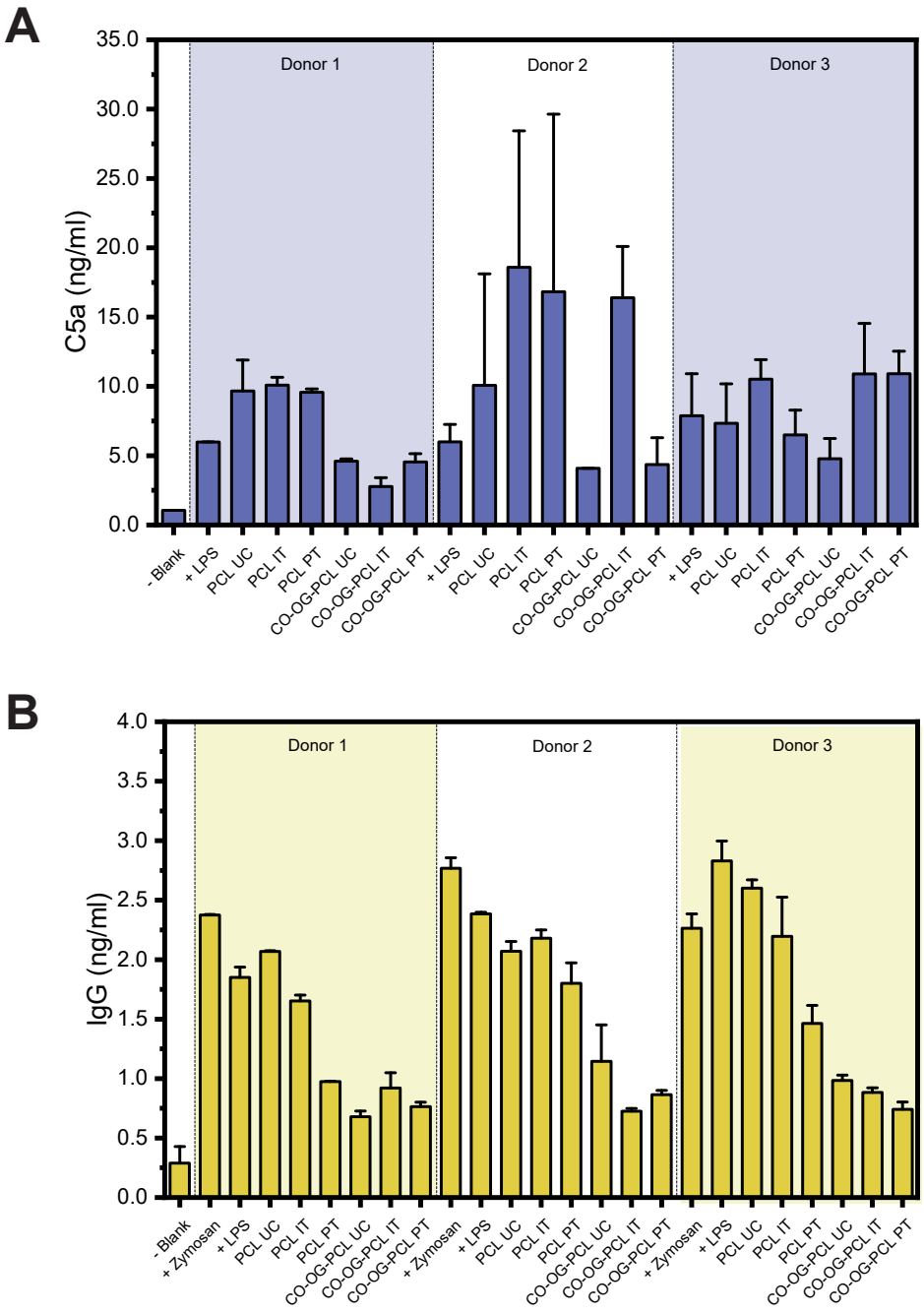

Figure 24 *C5a and IgG activation per condition per donor.*
A *C5a activation per donor per condition. Donor 2 had attenuated responses and larger error margins.* ***B*** *IgG activation per condition per donor. No large differences were found between donors.*